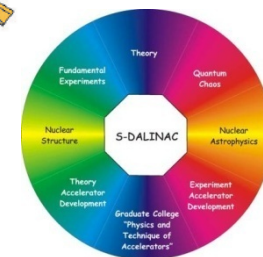
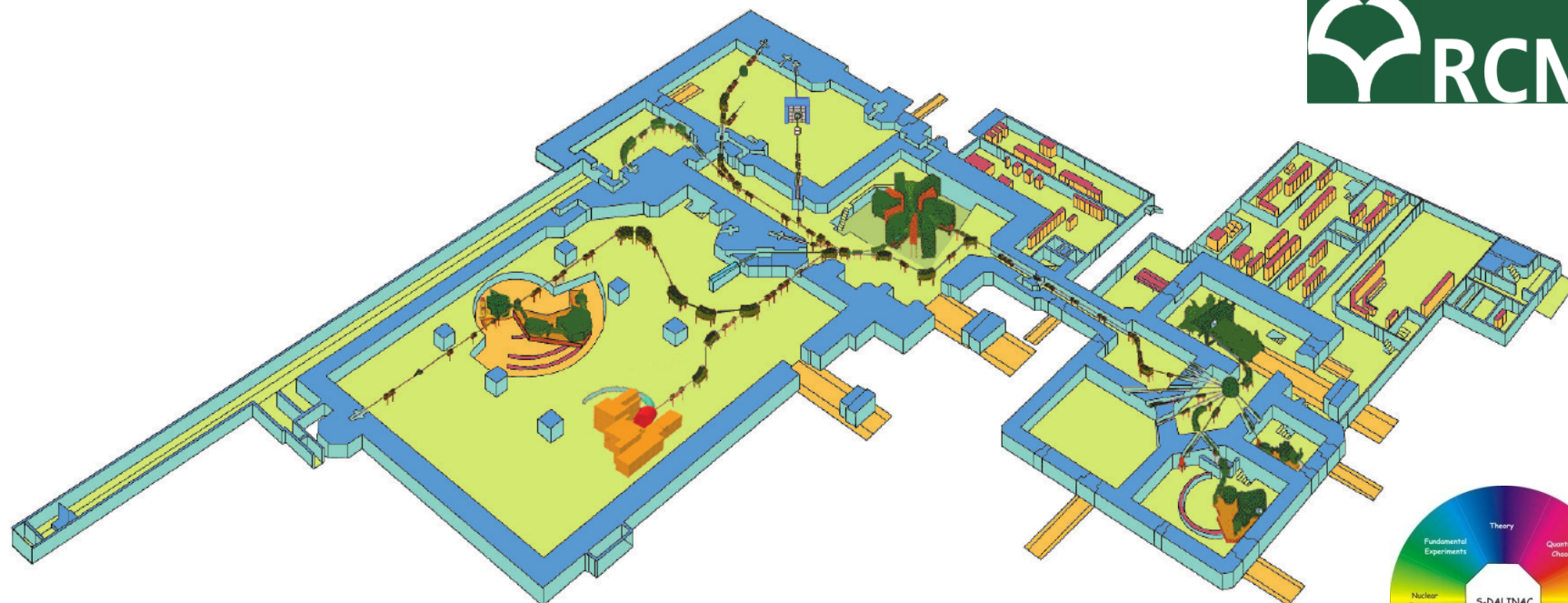


# Do we understand Gamma Strength Functions? The case of $^{96}\text{Mo}^*$



TECHNISCHE  
UNIVERSITÄT  
DARMSTADT

4th Workshop on Nuclear Level Density and Gamma Strength  
Dirk Martin for the E376 collaboration



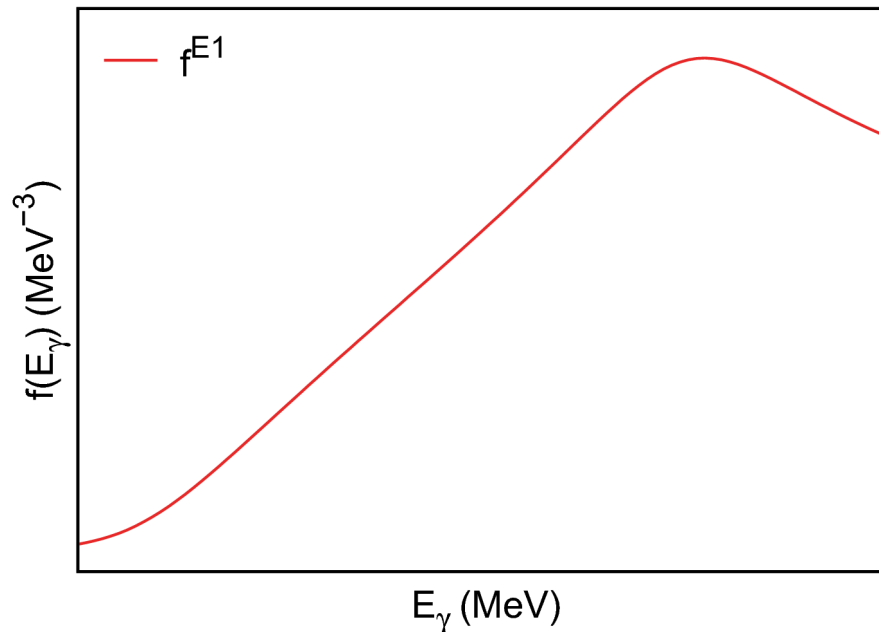
\*Supported by the DFG through SFB 634 and NE679/3-1

- ▶ Gamma Strength Function and Axel-Brink Hypothesis
- ▶ Polarized proton scattering at  $0^\circ$
- ▶ Data analysis
- ▶ First results
- ▶ Summary and outlook

# Gamma Strength Function (GSF)

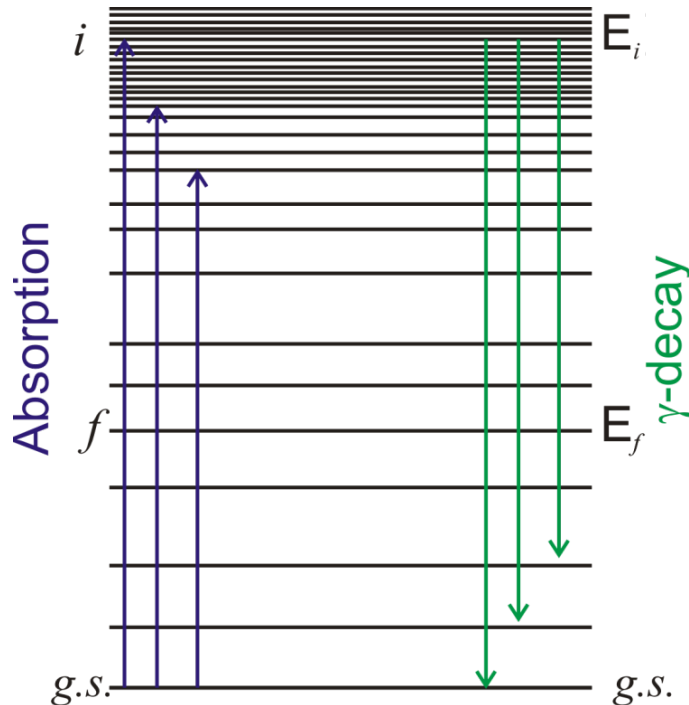
- ▶ Describes the (average) energy distribution of photon emission from highly-excited states or cross section for photon absorption

$$\langle \Gamma(E_i) \rangle \propto \sum_{X\lambda} \int_0^{E_i} E_\gamma^{2L+1} \frac{f^{X\lambda}(E_\gamma) \rho(E_f)}{\rho(E_i)} dE_\gamma$$



# Gamma Strength Function (GSF)

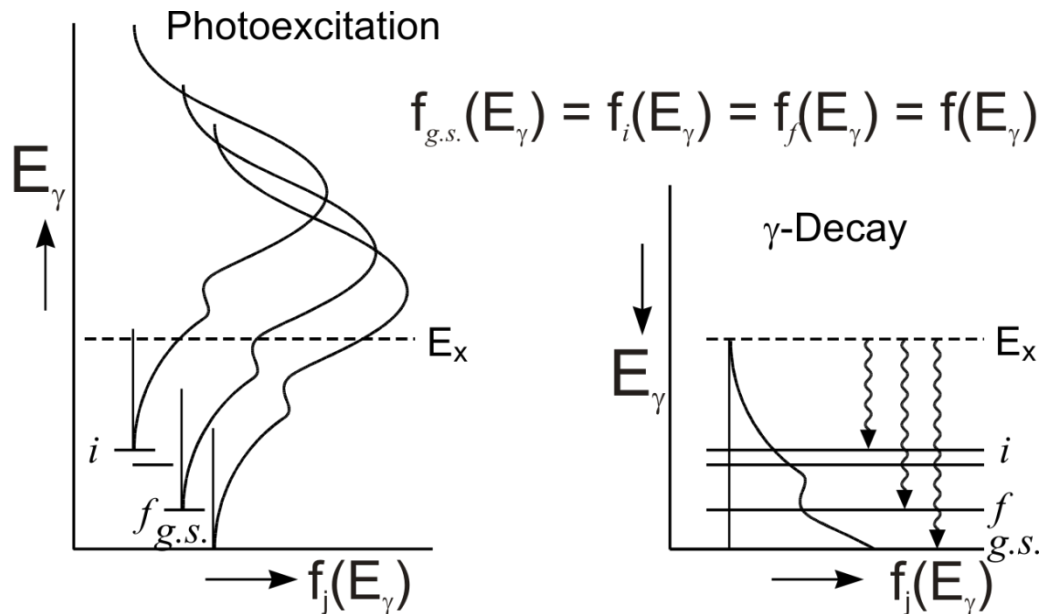
- ▶ Principle of detailed balance:



$$\langle \Gamma_{i \rightarrow g.s.} \rangle = \frac{f^{E1}(E_\gamma) \cdot E_\gamma^3}{\rho(E_i)}$$

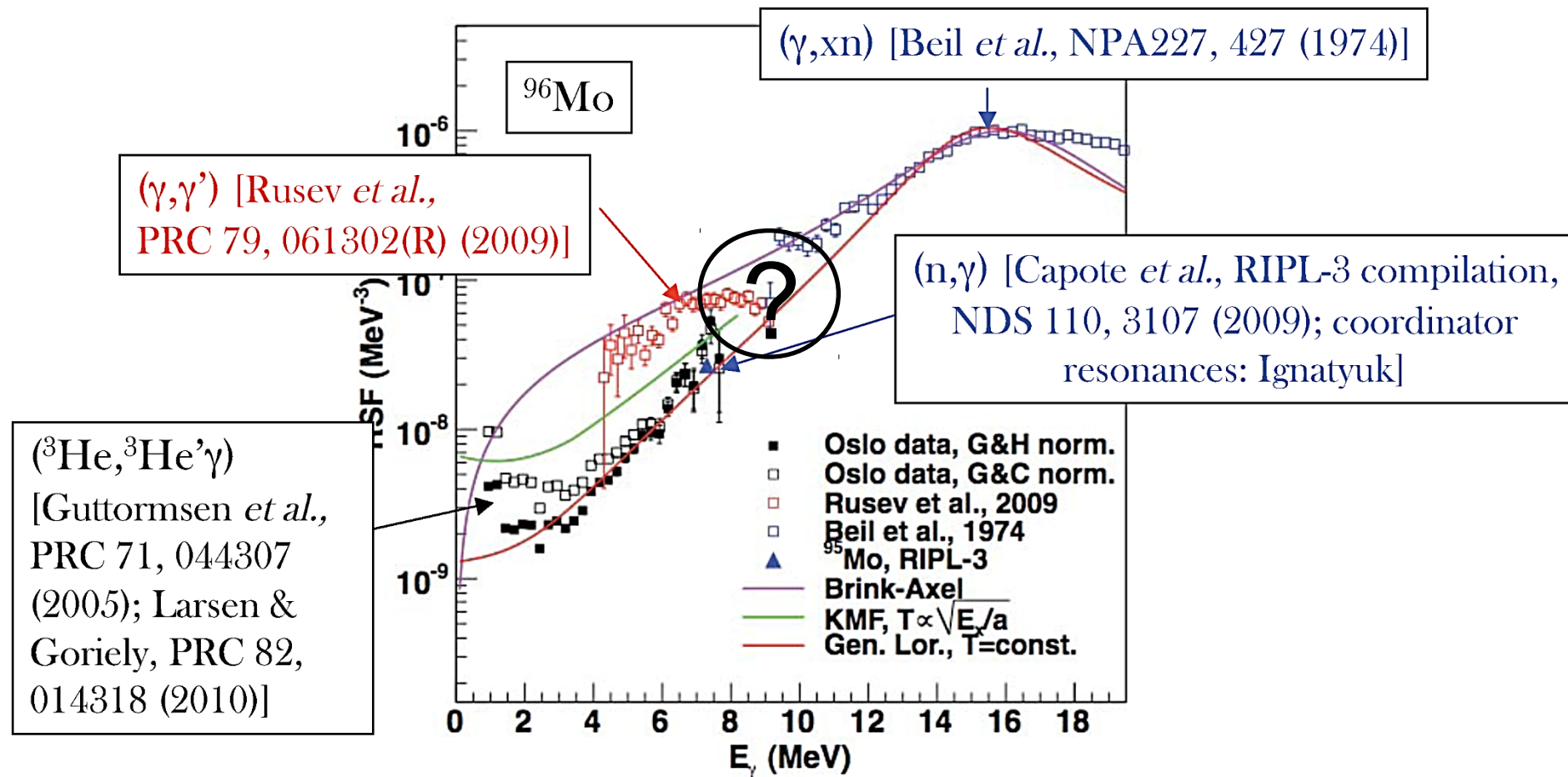
$$f^{E1}(E_\gamma) = \frac{\sigma_{abs}(E_i)}{3(\pi\hbar c)^2 \cdot E_\gamma}$$

# Axel-Brink Hypothesis



- ▶ Gamma Strength Function:
  - only depends on  $E_\gamma$
  - is independent of the initial state structure: excitation energy  $E_x$ ,  $J^\pi, \dots$
- ▶ Same GSF for absorption and gamma emission
- ▶ Used for correction of stellar cross sections due to thermal population of excited states

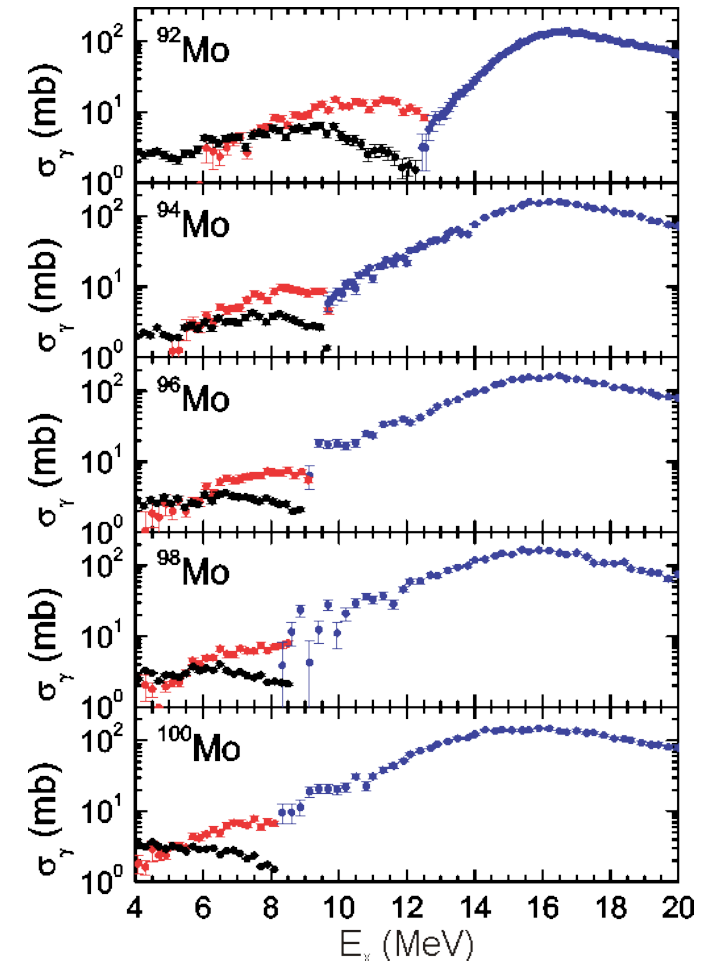
# Experimental discrepancies in GSF



Ann-Cecilie Larsen, 3rd Workshop on Level Density and Gamma Strength, Oslo, Norway, May 23 — 27, 2011

# Experimental problems

- ▶  $(\gamma, \gamma')$  experiments:
  - Measure strength up to neutron threshold only
  - Experimental quantity  $\Gamma_0 \cdot \frac{\Gamma_0}{\Gamma}$
  - Assumption in most analyses:  $\frac{\Gamma_0}{\Gamma} = 1$ 
    - ➔ lower limit
  - Alternatively: correction with statistical model calculations
    - ➔ upper limit



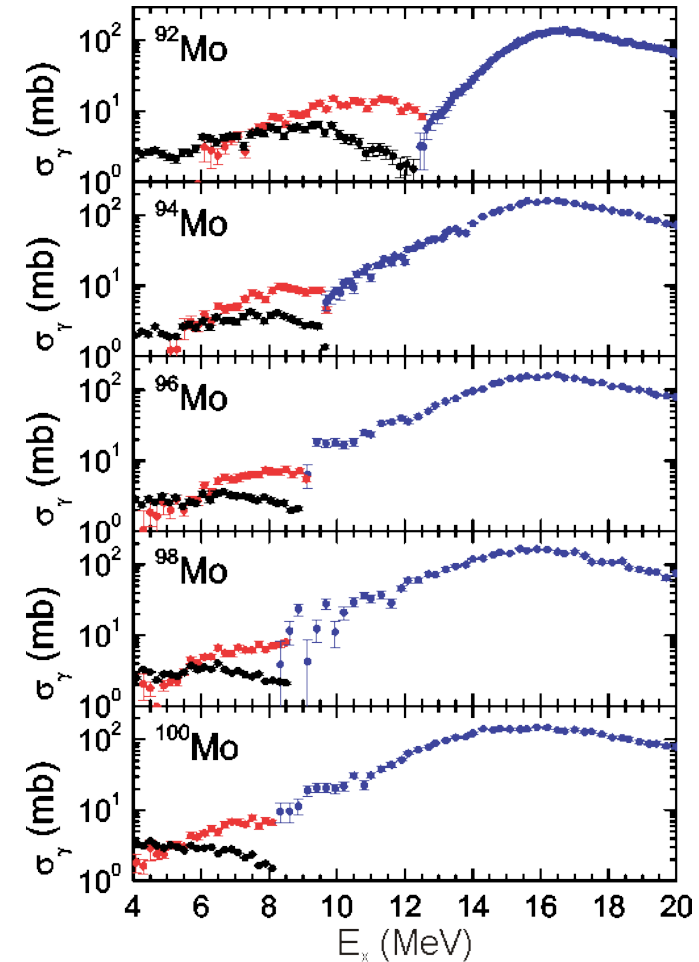
[G. Rusev et al., PRC **79** (2009) 061302]

# Experimental problems (continued)

- ▶  $(\gamma, xn)$  reactions provide information only above threshold
- ▶ Decay reactions:
  - Normalization at the  $S_n$  energy
  - Level densities needed



Consistent data on strength below and above the neutron threshold highly important!



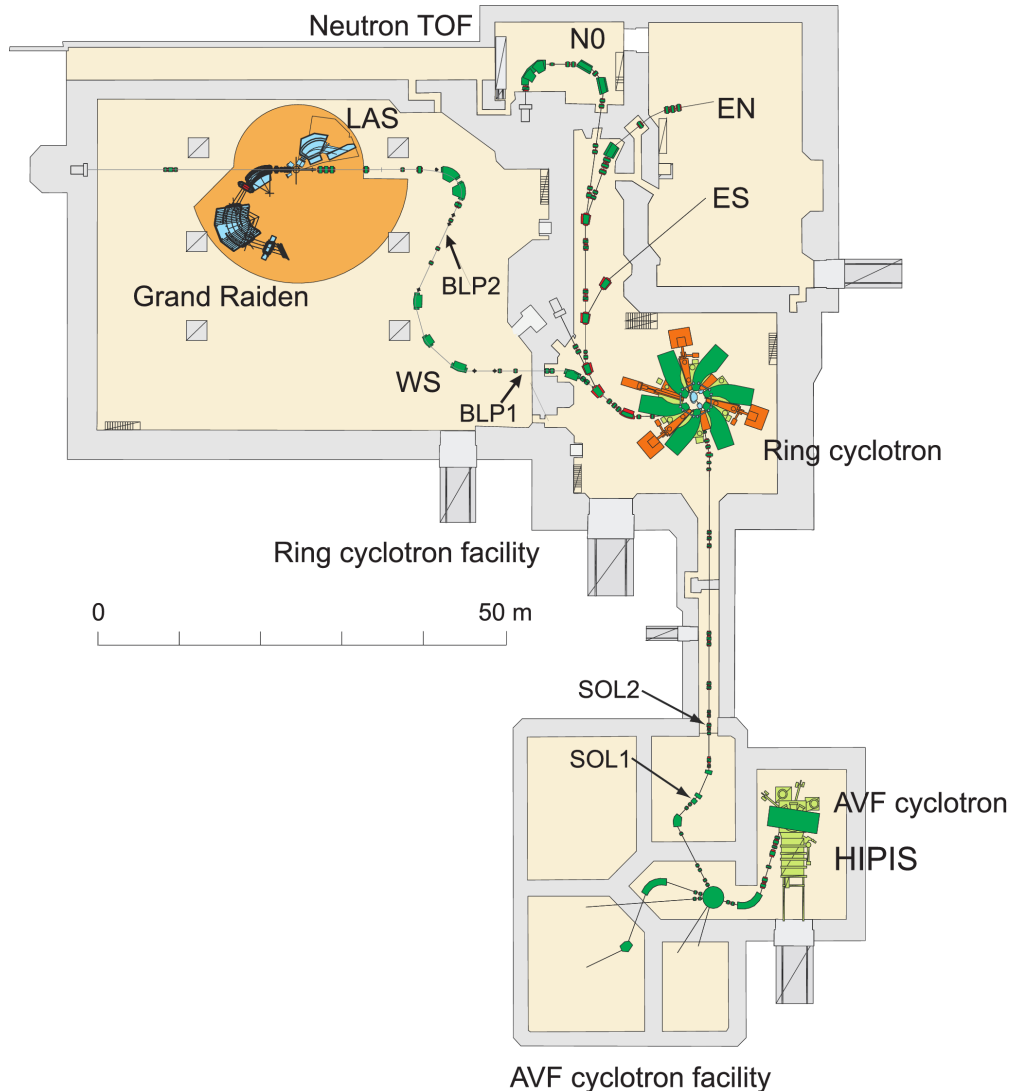
[G. Rusev et al., PRC **79** (2009) 061302]



# Complete E1 and M1 strength distributions

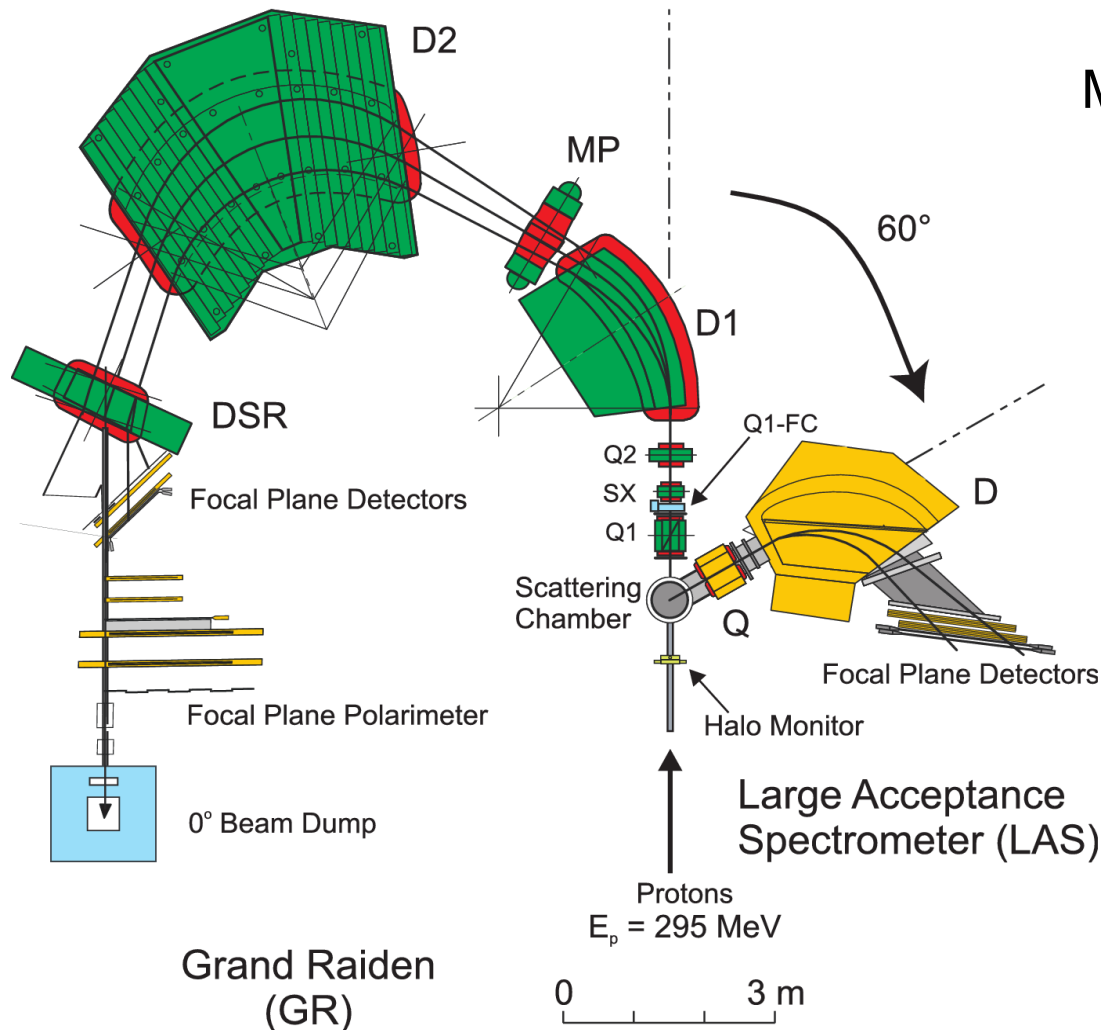
- ▶ Polarized proton scattering at  $0^\circ$ 
  - Intermediate energy: 300 MeV optimal
  - High energy resolution:  $\Delta E = 25\text{-}30$  keV (FWHM)
  - Angular distributions: E1 / M1 separation via multipole decomposition analysis
  - Polarization observables: spinflip / non-spinflip separation
  
- ▶  $^{208}\text{Pb}$  as a reference case (I. Poltoratska, doctoral thesis)
- ▶ Low-energy dipole modes in the heavy deformed nucleus  $^{154}\text{Sm}$
- ▶ Complete dipole response in  $^{120}\text{Sn}$

# Research Center for Nuclear Physics (RCNP) in Osaka, Japan



- ▶  $E_p = 295 \text{ MeV}$
- ▶ Beam intensity: 1-2 nA
- ▶ Dispersion matching:  
 $\Delta E = 25\text{-}30 \text{ keV}$
- ▶ Polarization:  $\sim 70\%$
- ▶ Beam polarization was periodically flipped to avoid instrumental asymmetries

# 0° setup at RCNP in Osaka



Measured observables for  $^{208}\text{Pb}$ :

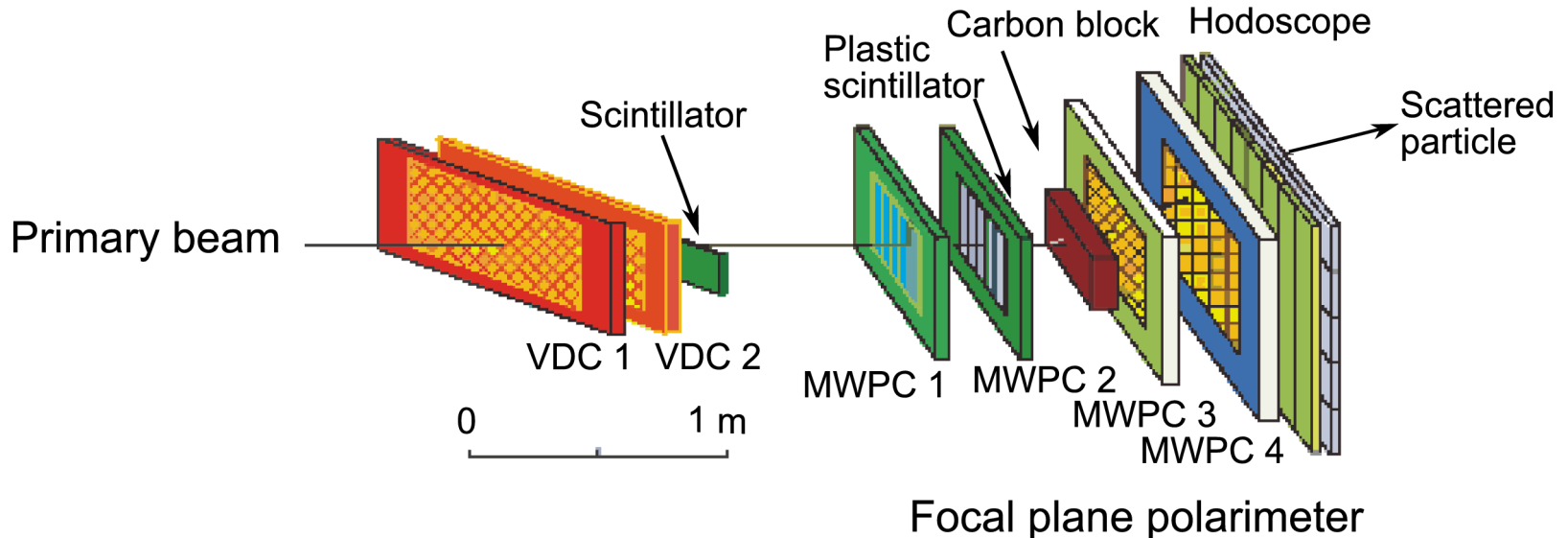
- ▶  $d\sigma^2/d\Omega dE$  @  $0^\circ, 2.5^\circ$
- ▶  $D_{SS}$  @  $0^\circ$  (sideways PT)
- ▶  $D_{LL}$  @  $0^\circ$  (longitudinal PT)

Small vertical magnification



Mild under-focus mode

# Grand Raiden detector system



- ▶ Focal plane detector system:

Determination of positions  $x_{fp}$ ,  $y_{fp}$   
and angles  $\theta_{fp}$ ,  $\phi_{fp}$

- ▶ Focal plane polarimeter:

Measurement of the polarization  $p''$  after a secondary scattering off a carbon slab

# E1/M1 decomposition by spin observables

Polarization observables at  $0^\circ$   $\longrightarrow$  **spinflip / non-spinflip separation\***  
(model-independent)

$$D_{SS} + D_{NN} + D_{LL} = \begin{cases} -1 & \text{for } \Delta S = 1 \\ 3 & \text{for } \Delta S = 0 \end{cases}$$

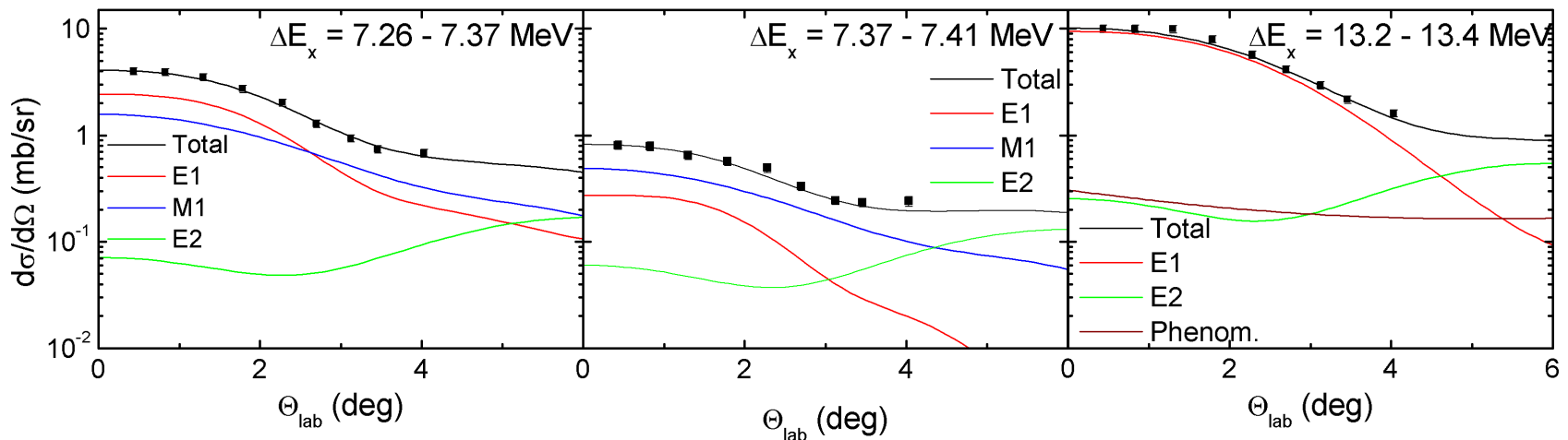
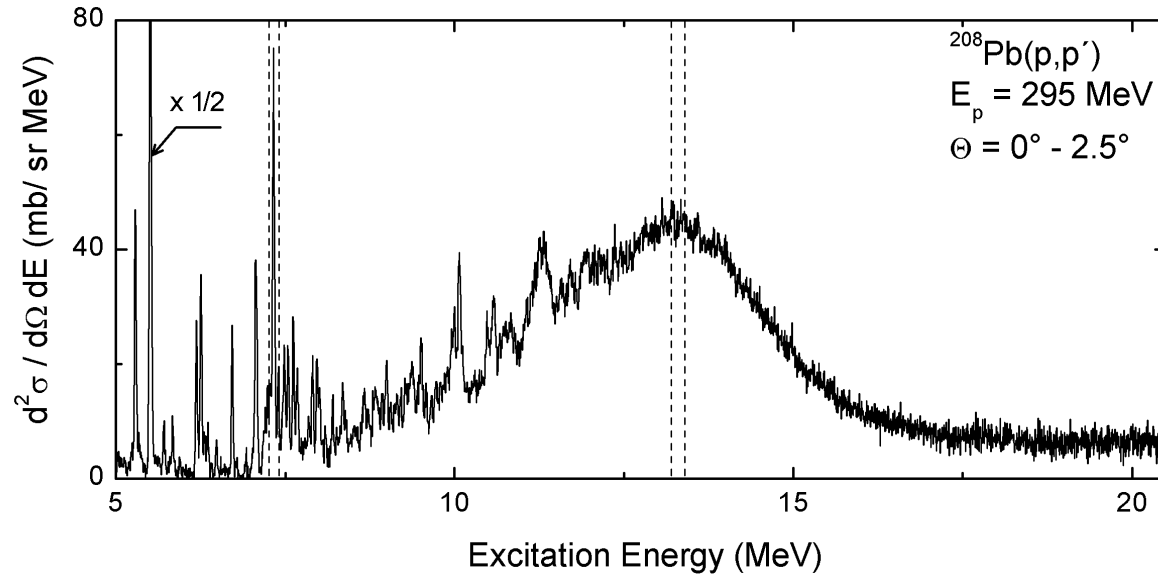
$\longrightarrow$  E1 and M1 cross sections can be decomposed

At  $0^\circ$ :  $D_{SS} = D_{NN}$

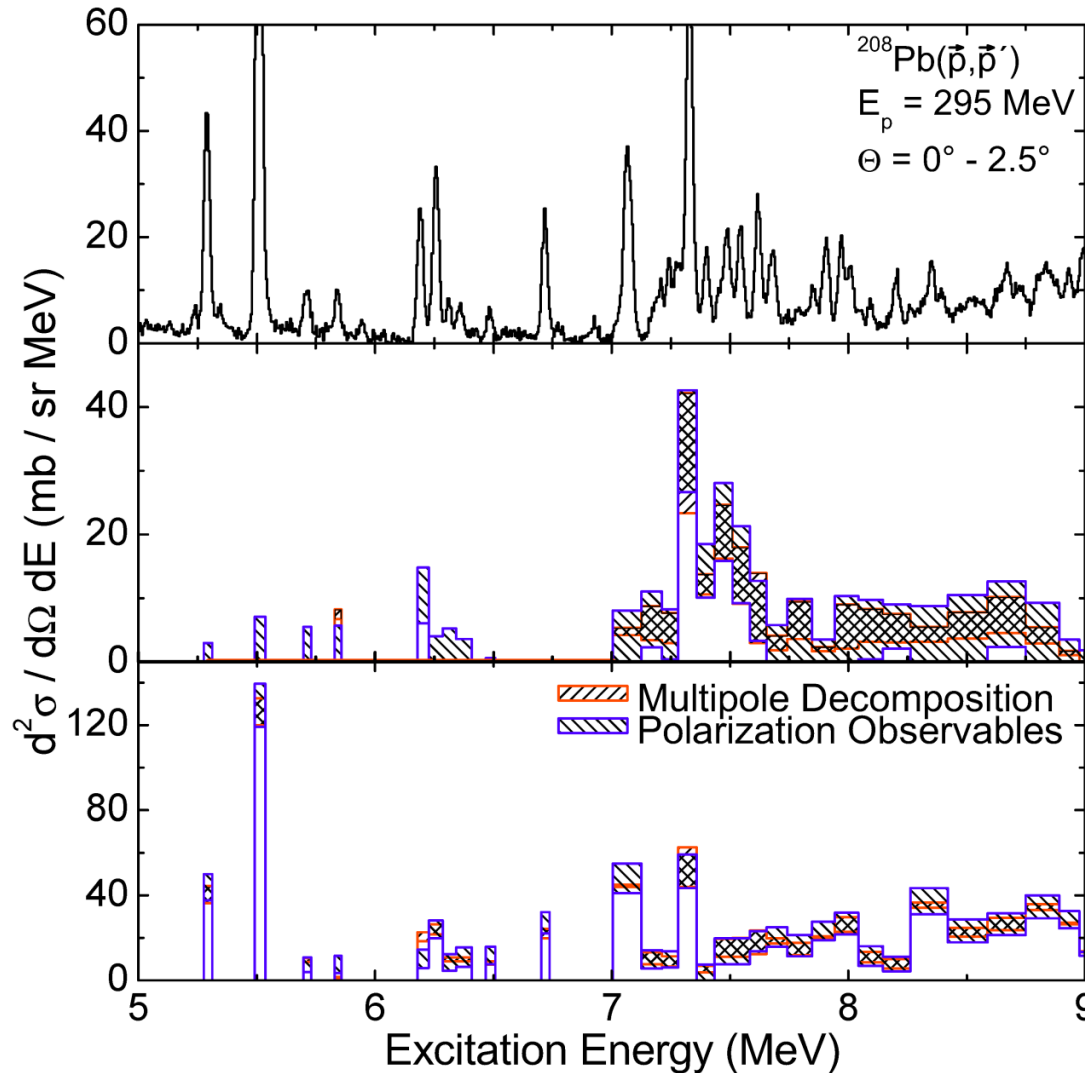
$$\text{Total Spin Transfer } \Sigma \equiv \frac{3 - (2D_{NN} + D_{LL})}{4} = \begin{cases} 1 & \text{for } \Delta S = 1 \quad \textbf{(M1)} \\ 0 & \text{for } \Delta S = 0 \quad \textbf{(E1)} \end{cases}$$

\* [T. Suzuki, Prog. Theo. Phys. **103** (2000) 859]

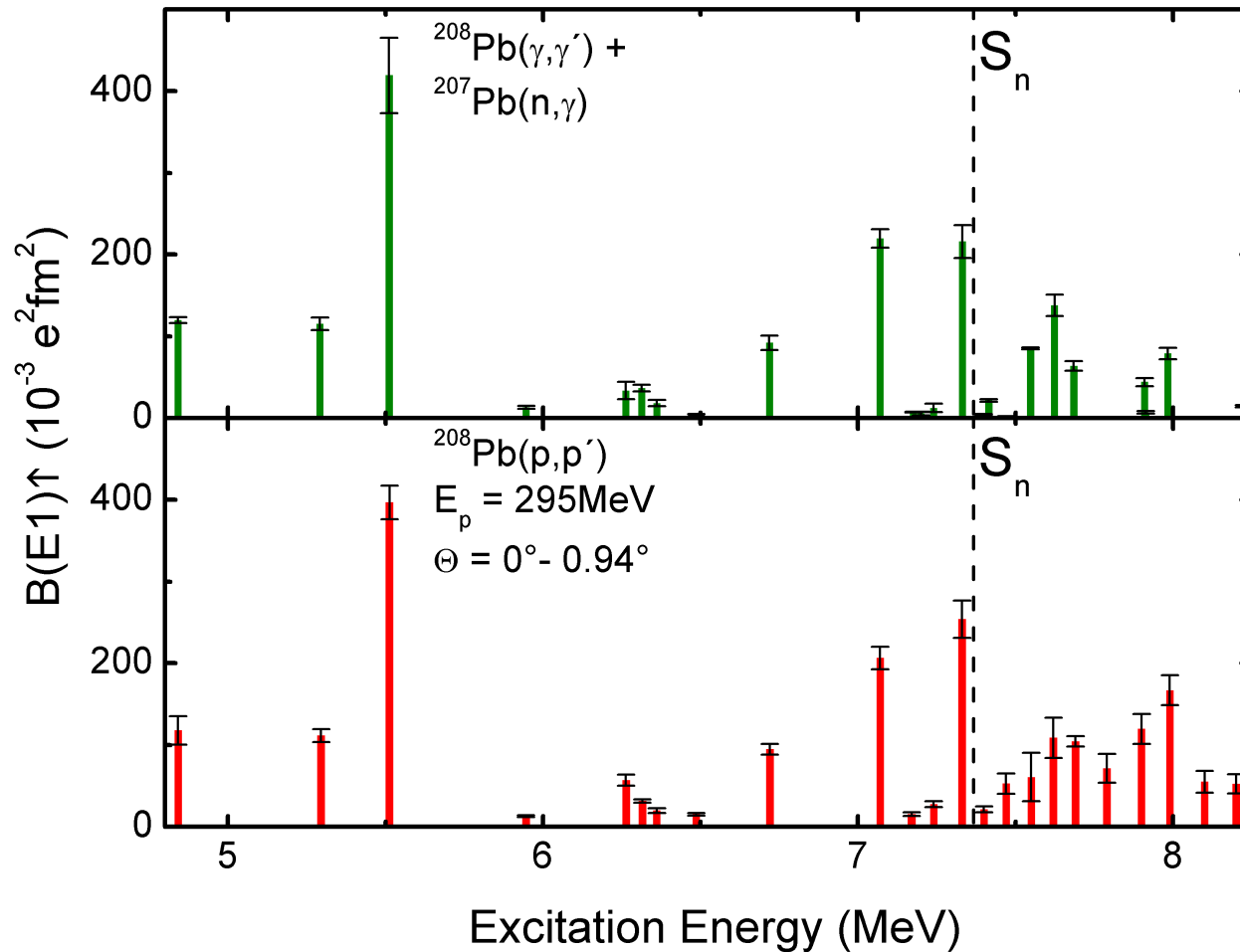
# Multipole decomposition of angular distributions



# Comparison of both methods for $^{208}\text{Pb}$

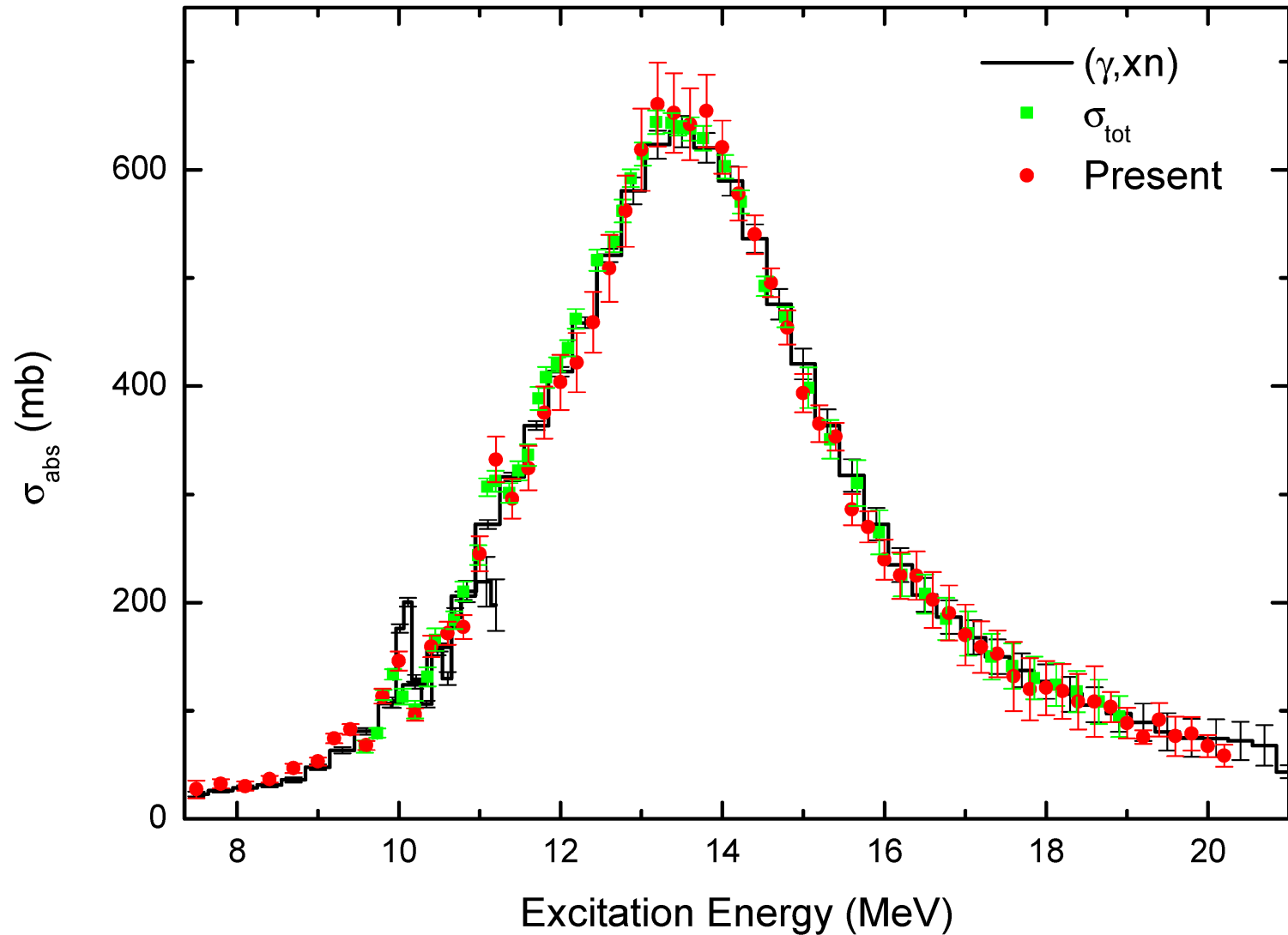


# B(E1) strength: low-energy region

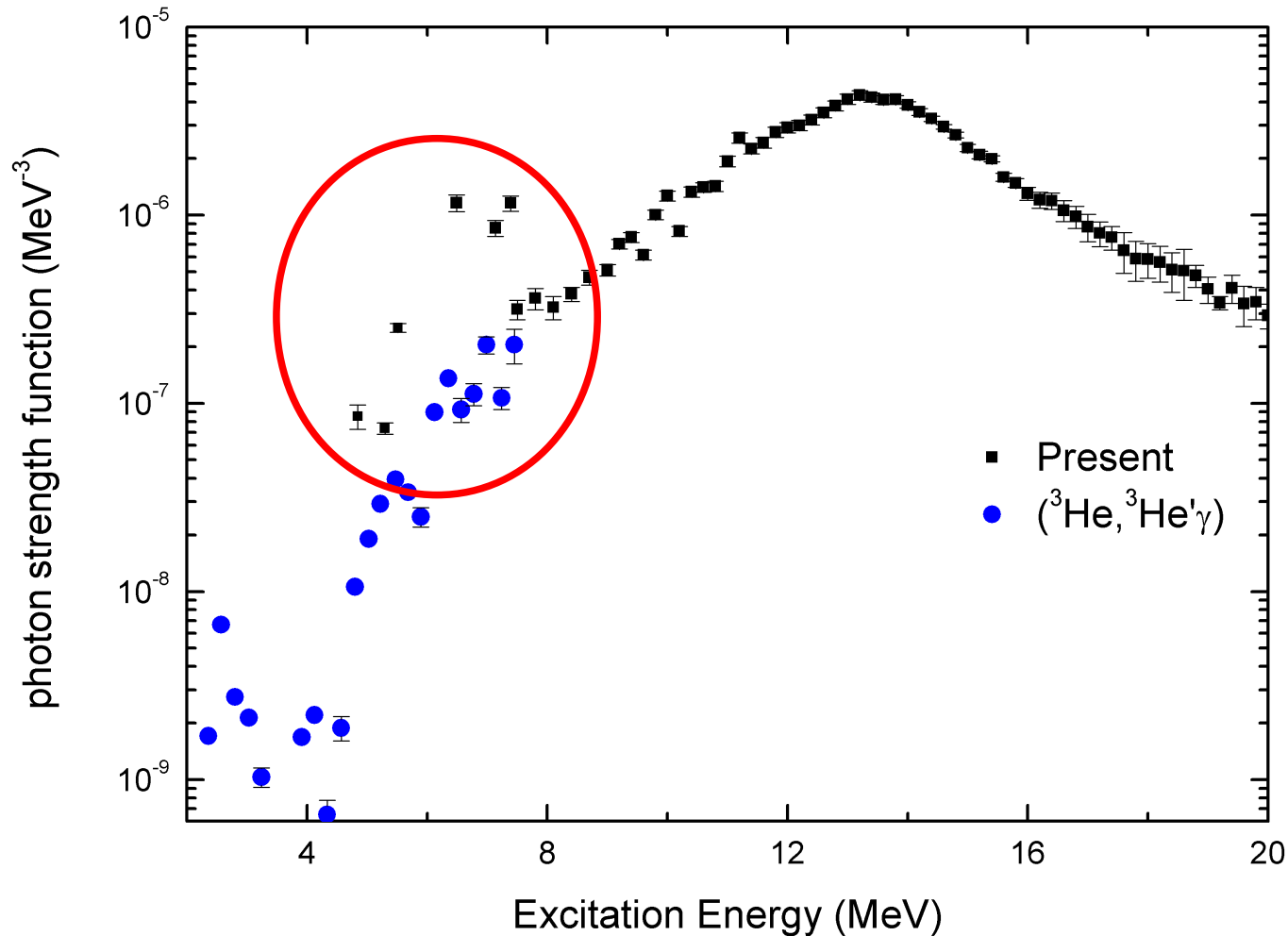




# Photoabsorption cross section of $^{208}\text{Pb}$

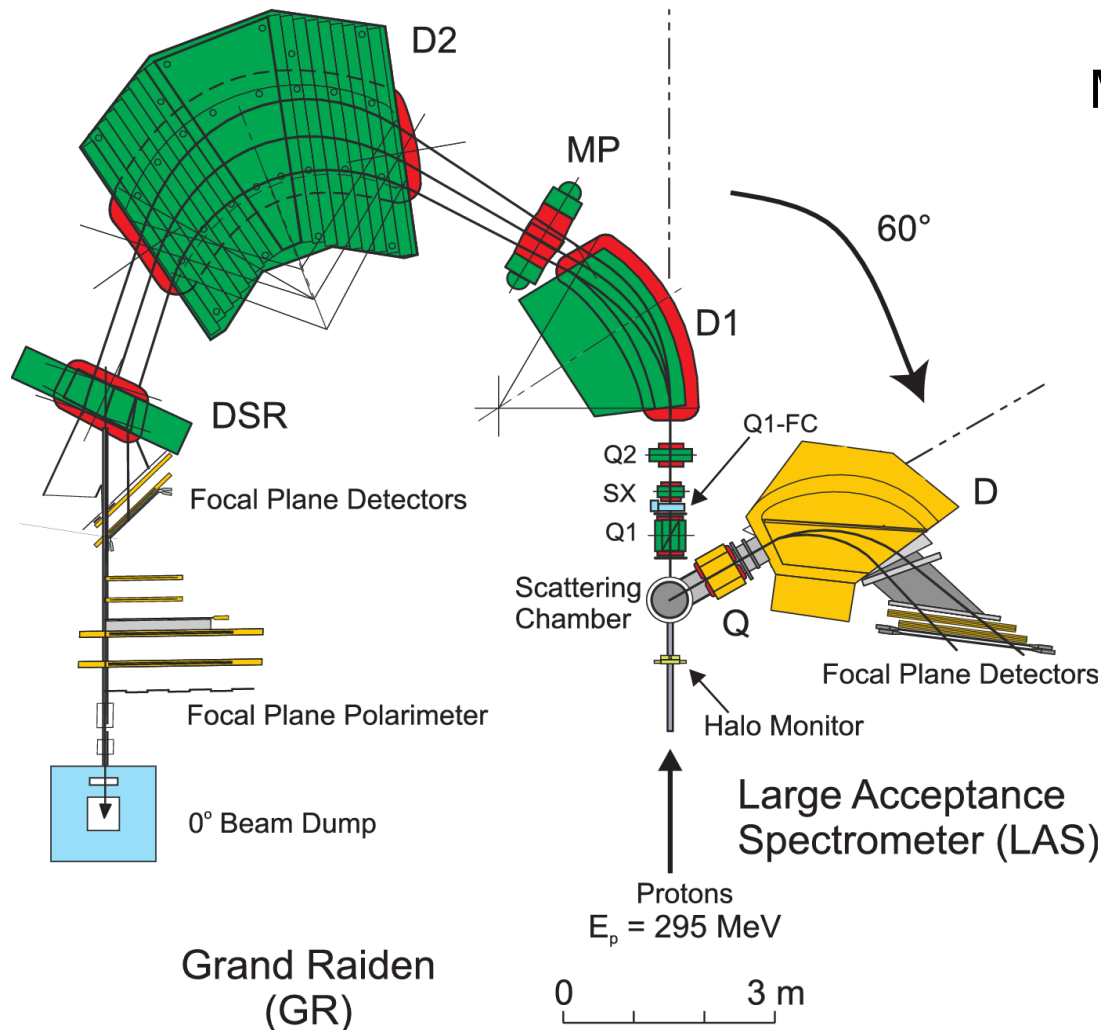


# Gamma Strength Function in $^{208}\text{Pb}$



► ( $^3\text{He}, ^3\text{He}'\gamma$ ) normalized to ( $n, \gamma$ ) data

# 0° setup at RCNP in Osaka



Measured observables for  $^{96}\text{Mo}$ :

- ▶  $d\sigma^2/d\Omega dE$  @  $0^\circ$ ,  $3^\circ$  and  $4.5^\circ$
- ▶  $D_{NN}$  @  $0^\circ$  (normal PT)
- ▶  $D_{LL}$  @  $0^\circ$  (longitudinal PT)

Small vertical magnification

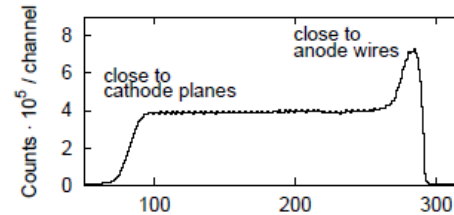


Mild under-focus mode

# Analysis steps



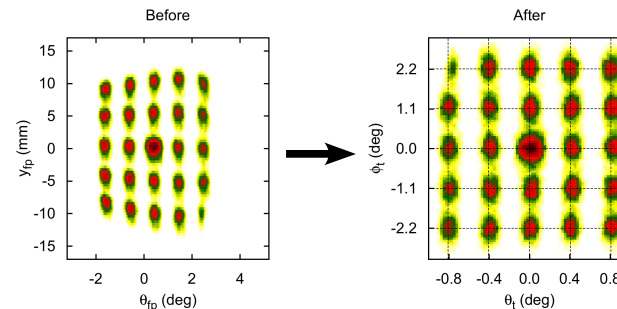
- ▶ Drift time to drift length conversion



- ▶ Determination of efficiency of VDCs

$$\epsilon_{total} = 88\%$$

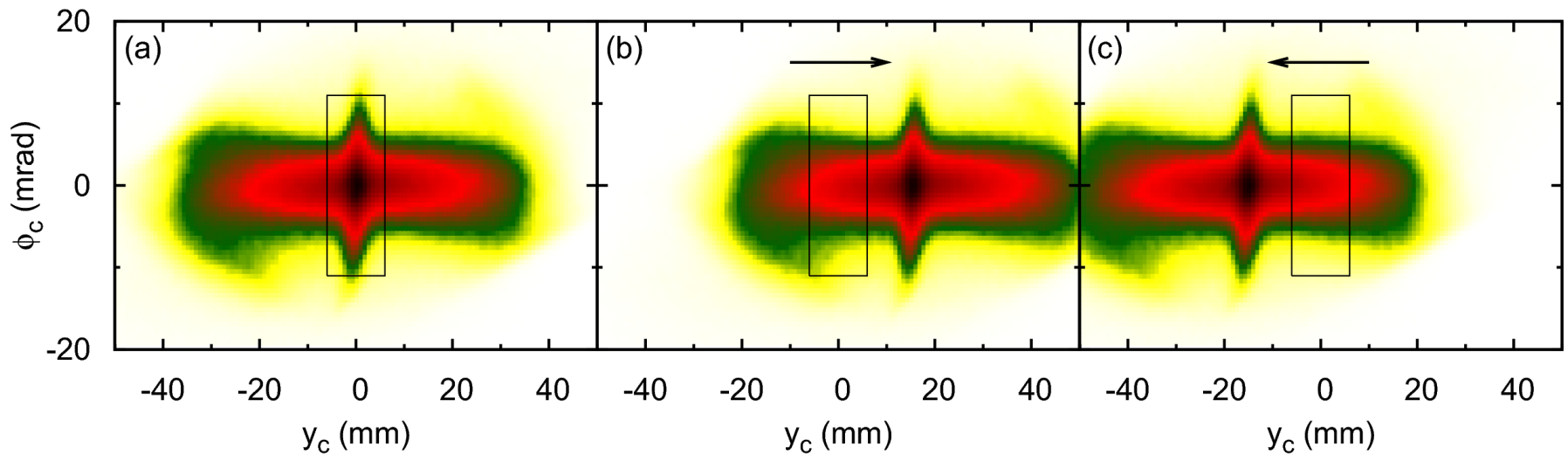
- ▶ Calibration of scattering angles



- ▶ High-resolution correction and excitation energy calibration

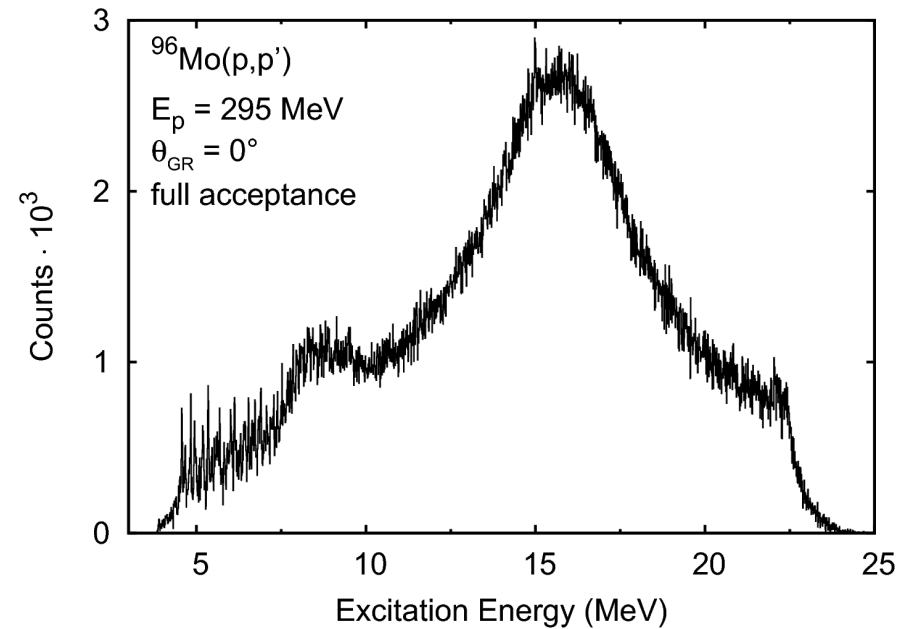
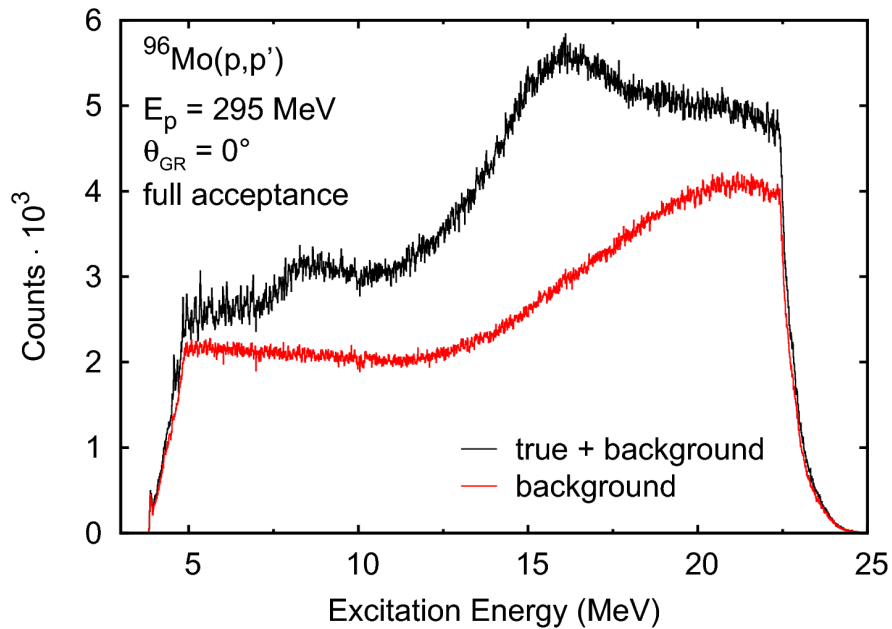
- $^{26}\text{Mg}$  runs before each  $^{96}\text{Mo}$  run
- Many prominent  $1^+$  states in  $^{26}\text{Mg}$
- Test of the polarization transfer analysis (spinflip M1 transitions)

# Background subtraction



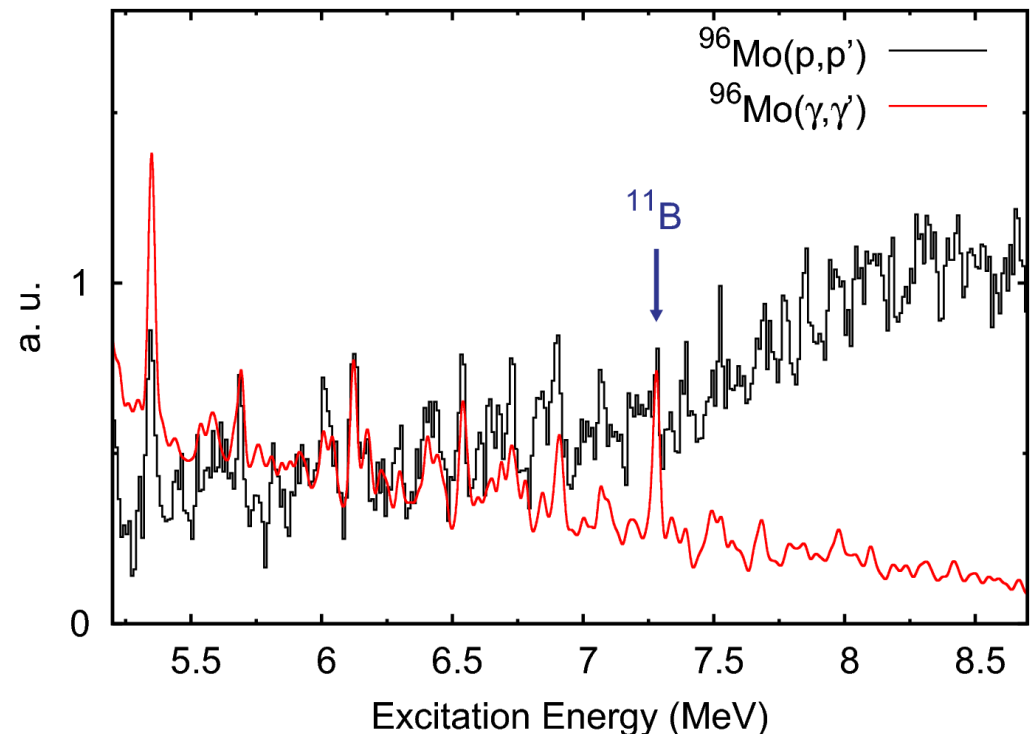
- ▶ Background events: flat distribution in non-dispersive focal plane
- ▶ True events focus at  $y_c = 0$

# Background subtraction



# Qualitative comparison to $(\gamma, \gamma')$ experiments

- ▶ Measured at the Helmholtz-Zentrum Dresden-Rossendorf
- ▶ Endpoint energy: 13.2 MeV
- ▶  $\theta = 127^\circ$
- ▶ Convolted with a Gaussian with  $\Delta E = 25$  keV
- ▶ Arbitrarily normalized to peaks between 6 MeV and 6.5 MeV



# Polarization transfer analysis

- ▶ Second scattering off a carbon slab (~9 cm thick):

$$p_N''^t = D_{NN} p_N$$

$$p_N''^b = p_N$$

$$p_S''^t = D_{SS} p_S \cos \chi_p + D_{LL} p_L \sin \chi_p$$

$$p_S''^b = p_S \cos \chi_p + p_L \sin \chi_p$$

- ▶ Spin precession angle  $\chi_p$  of the GR spectrometer
- ▶  $p_L$ ,  $p_S$  and  $p_N$ : longitudinal, sideways and normal beam polarization
- ▶ Background events do not contribute to the depolarization, i.e.  
 $D_{NN} = D_{SS} = D_{LL} = 1$



- ▶ Estimator for measured asymmetries after secondary scattering:

$$\varepsilon_N^t = \rho_N''^t \langle A_y \rangle^{FPP}$$

$$\varepsilon_N^b = \rho_N''^b \langle A_y \rangle^{FPP}$$

$$\varepsilon_S^t = \rho_S''^t \langle A_y \rangle^{FPP}$$

$$\varepsilon_S^b = \rho_S''^b \langle A_y \rangle^{FPP}$$



$$\frac{\varepsilon_N^t}{\varepsilon_N^b} = \frac{D_{NN}\rho_N}{\rho_N} = D_{NN}$$
$$\frac{\varepsilon_S^t}{\varepsilon_S^b} = \frac{D_{SS}\rho_S \cos \chi_p + D_{LL}\rho_L \sin \chi_p}{\rho_S \cos \chi_p + \rho_L \sin \chi_p}$$
$$D_{NN} = D_{SS} \quad (\text{at } 0^\circ)$$

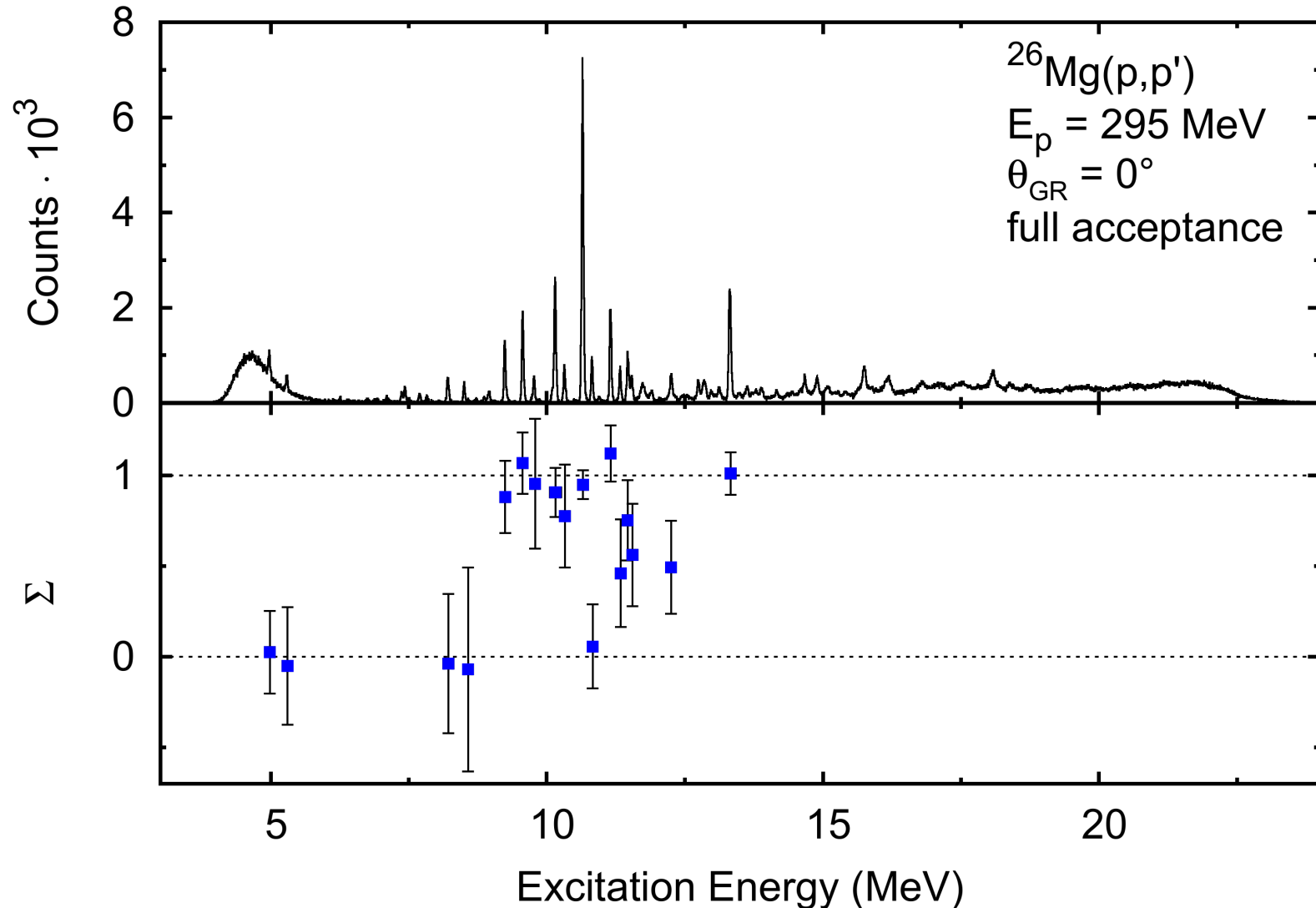
- ▶ Close to maximum use of data (compared to sector method e.g.)
- ▶ Calculation of uncertainties with covariance matrix
- ▶ Statistical treatment is well-defined and clear

[D. Besset et al., Nucl. Instr. Meth. **166** (1979) 515]

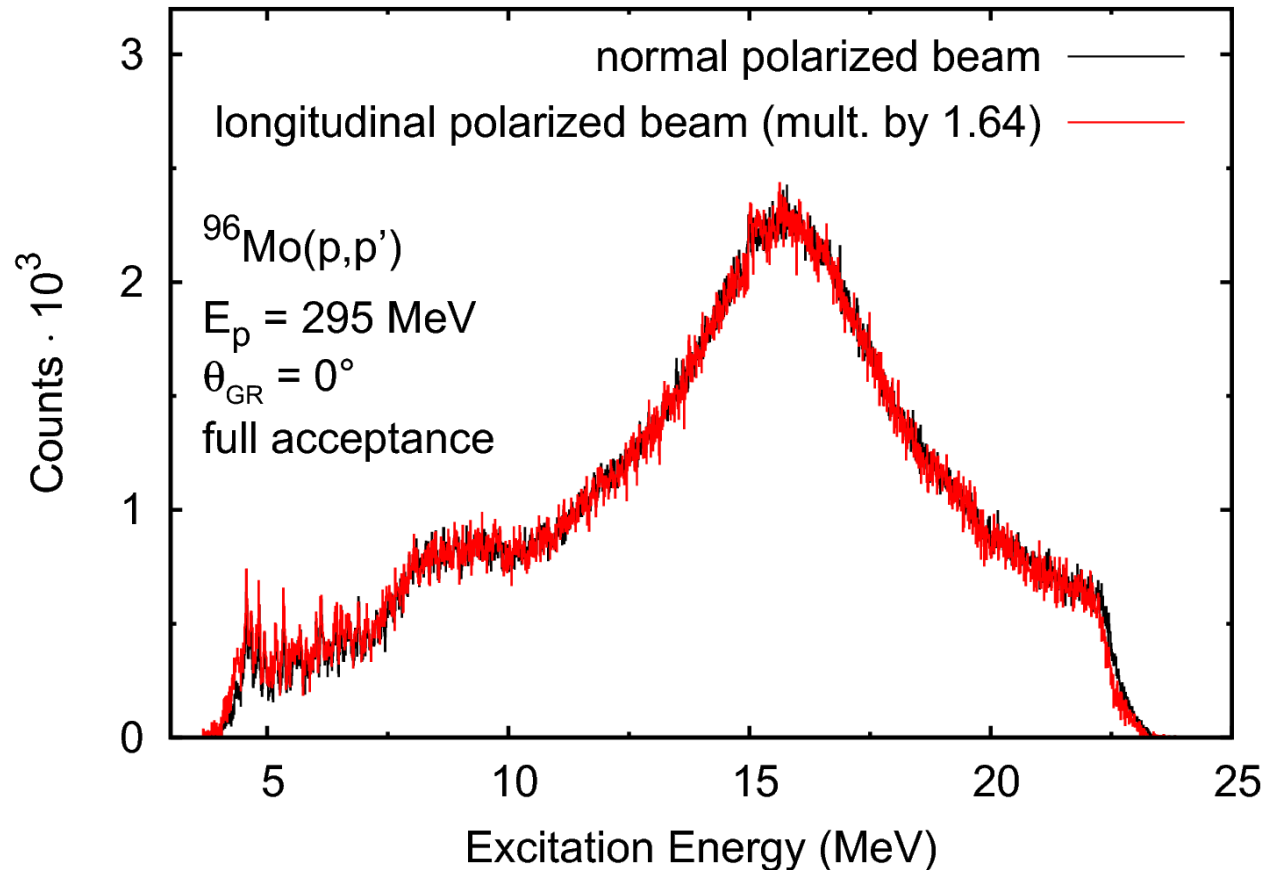
# Polarization transfer observables in $^{26}\text{Mg}$



TECHNISCHE  
UNIVERSITÄT  
DARMSTADT



# Consistency check of both polarization transfer measurements

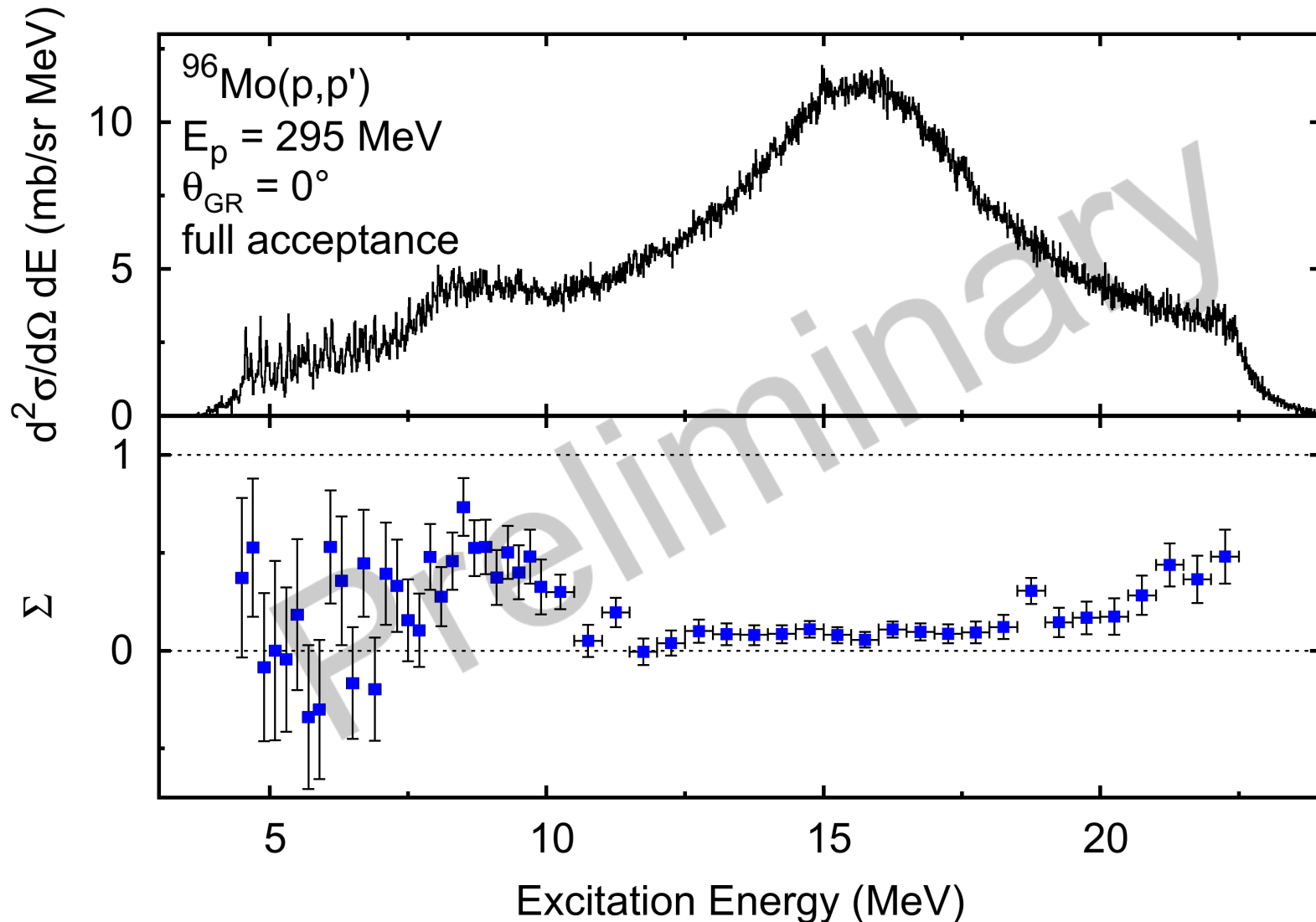


$$\Sigma = \frac{3 - (2D_{NN} + D_{LL})}{4}$$

# Polarization transfer observables in $^{96}\text{Mo}$

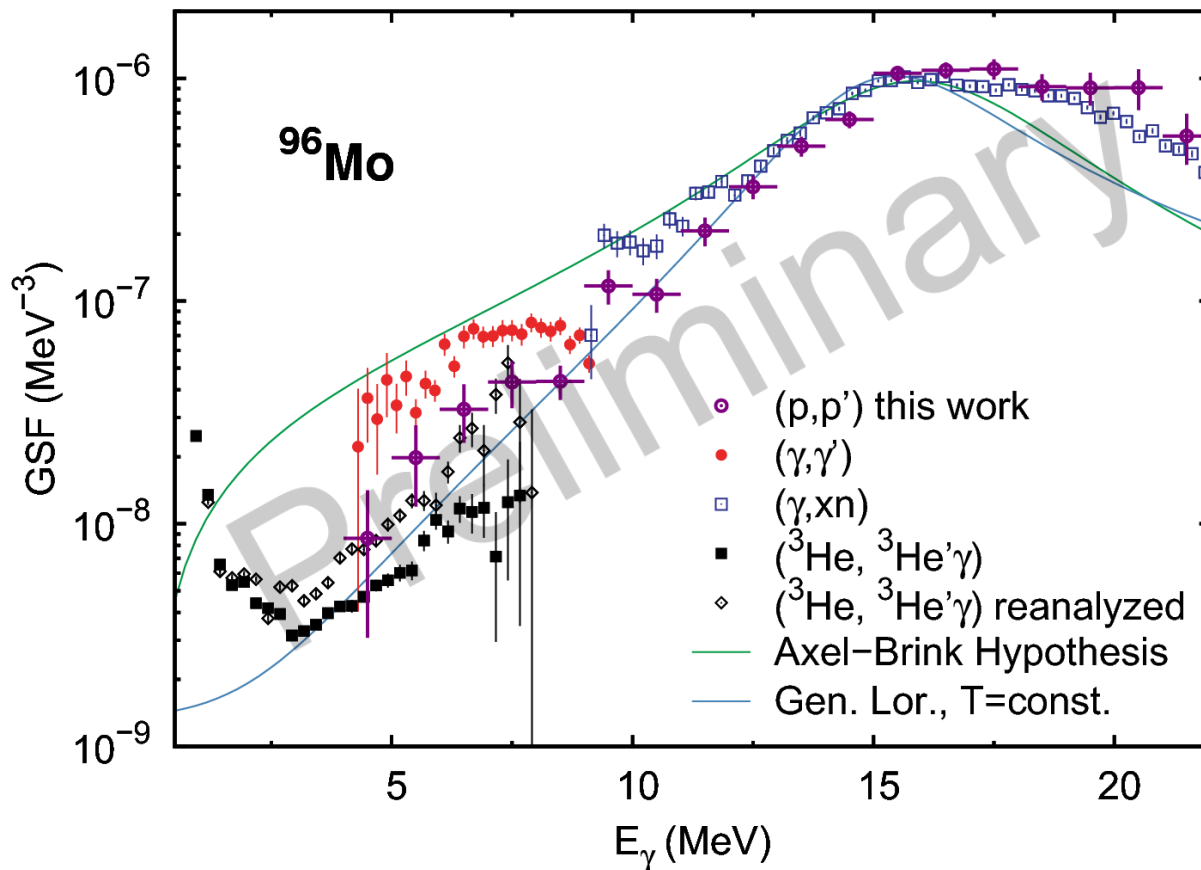


TECHNISCHE  
UNIVERSITÄT  
DARMSTADT



# Gamma Strength Function of $^{96}\text{Mo}$

- Gating on very forward angles  $\theta_t$  and  $\phi_t$ :  $\sum_{X\lambda} f^{X\lambda}(E_\gamma) \approx \sum_X f^{X\lambda=1}(E_\gamma)$



- ▶ Gamma Strength Function and Axel-Brink hypothesis
- ▶ Incompatible experimental data for  $^{96}\text{Mo}$
- ▶ Polarized proton scattering at  $0^\circ$  as the tool to study the GSF below and above the threshold
- ▶ Two different methods to extract E1 and M1 strength
  - Multipole decomposition analysis
  - Polarization transfer observables
- ▶ Preliminary results: polarization transfer observable analysis and GSF

- ▶ Angular distribution for multipole decomposition analysis (defining scattering angle cuts for measurements at  $0^\circ$ ,  $3^\circ$  and  $4.5^\circ$ )
- ▶ Compare GSF deduced from absorption and decay experiments
- ▶ Check of Axel-Brink Hypothesis
- ▶ Extraction of level densities

# Thank you for your attention!



TECHNISCHE  
UNIVERSITÄT  
DARMSTADT

## E376 Collaboration:

### **Miyazaki University**

Y. Maeda

### **Niigata University**

M. Nagashima, Y. Shimbara

### **Istanbul University**

B. Bilgier, E. Ganioglu,  
C. Kozer

### **iThemba LABS**

R. Neveling, M. Wiedeking,  
I. Usman

### **Univ. of Witwatersrand**

J. Carter, L. Donaldson

### **Kyoto University**

T. Kawabata

### **RIKEN**

J. Lee, H. Matsubara, J. Zenihiro

### **RCNP, Osaka University**

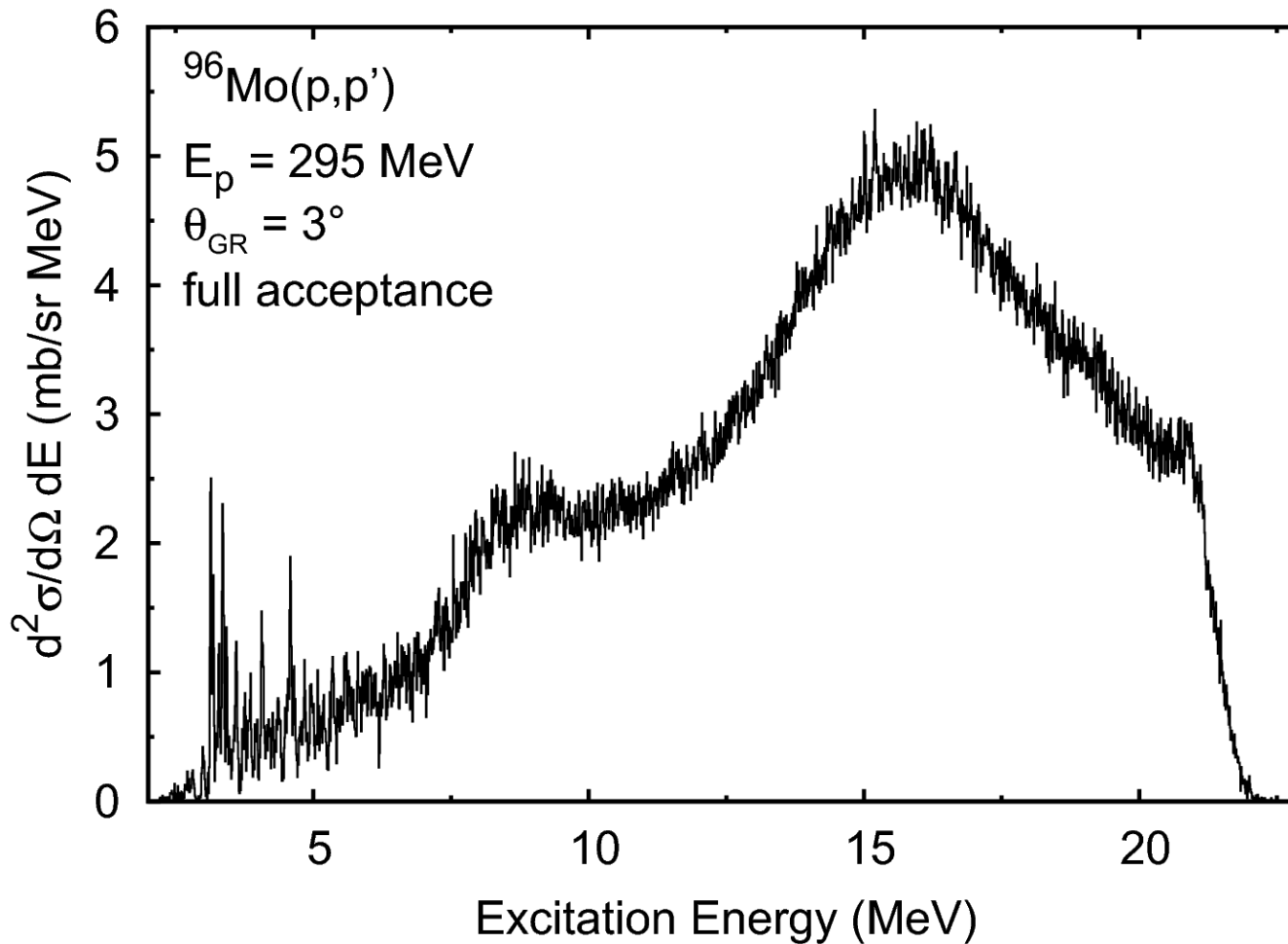
N. Aoi, H. Fujita, Y. Fujita, K. Hatanaka,  
T. Hashimoto, T. Itoh, B. Liu, K. Miki,  
H.-J. Ong, H. Sakaguchi, T. Shima,  
T. Suzuki, A. Tamii, M. Yosoi

### **IKP, TU Darmstadt**

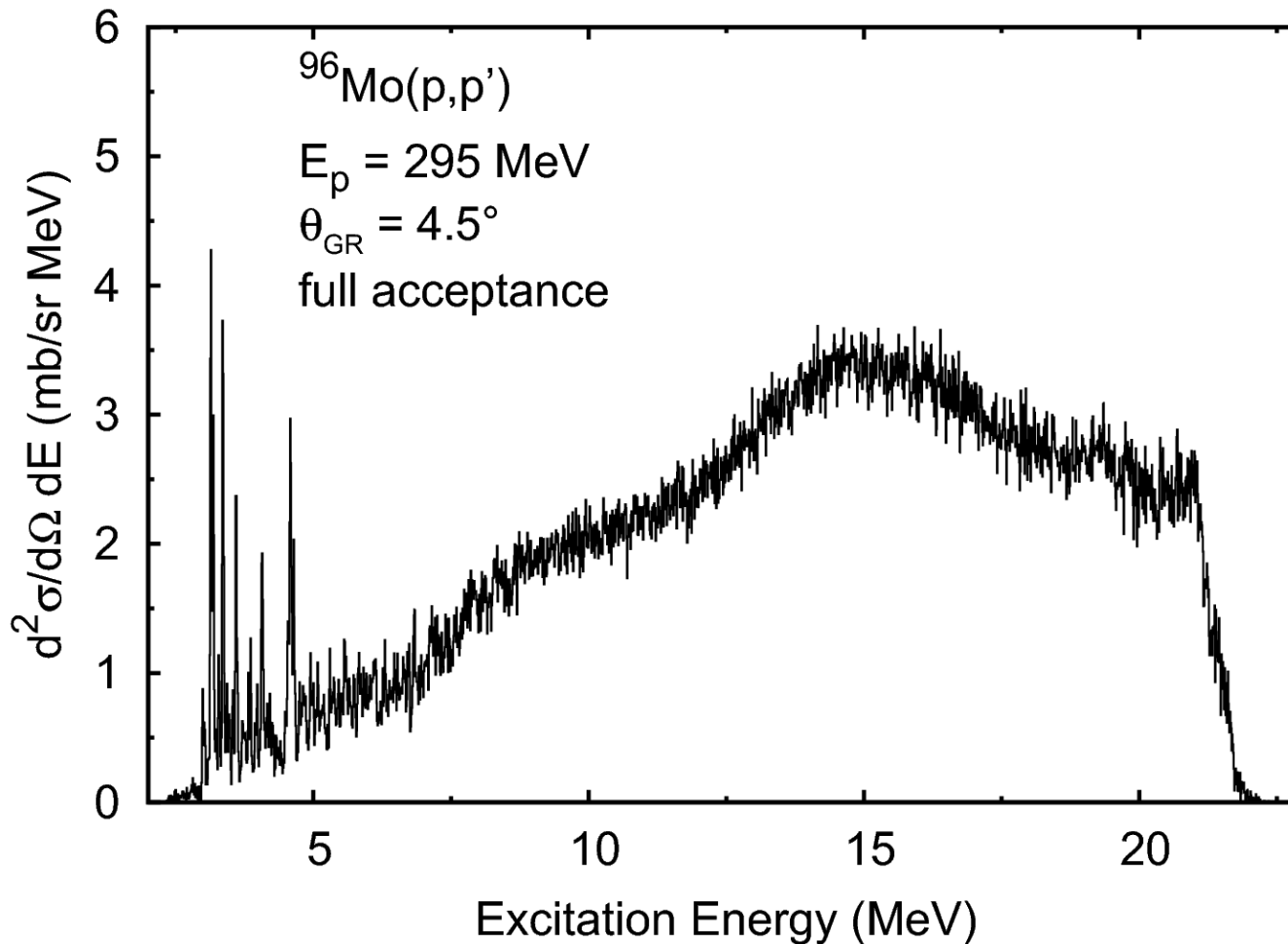
A. Ebert, A. Krugmann, A. M. Krumbholz,  
D. Martin, P. von Neumann-Cosel, N. Pietralla,  
I. Poltoratska, V. Yu. Ponomarev, A. Richter,  
J. Wambach, M. Zweidinger



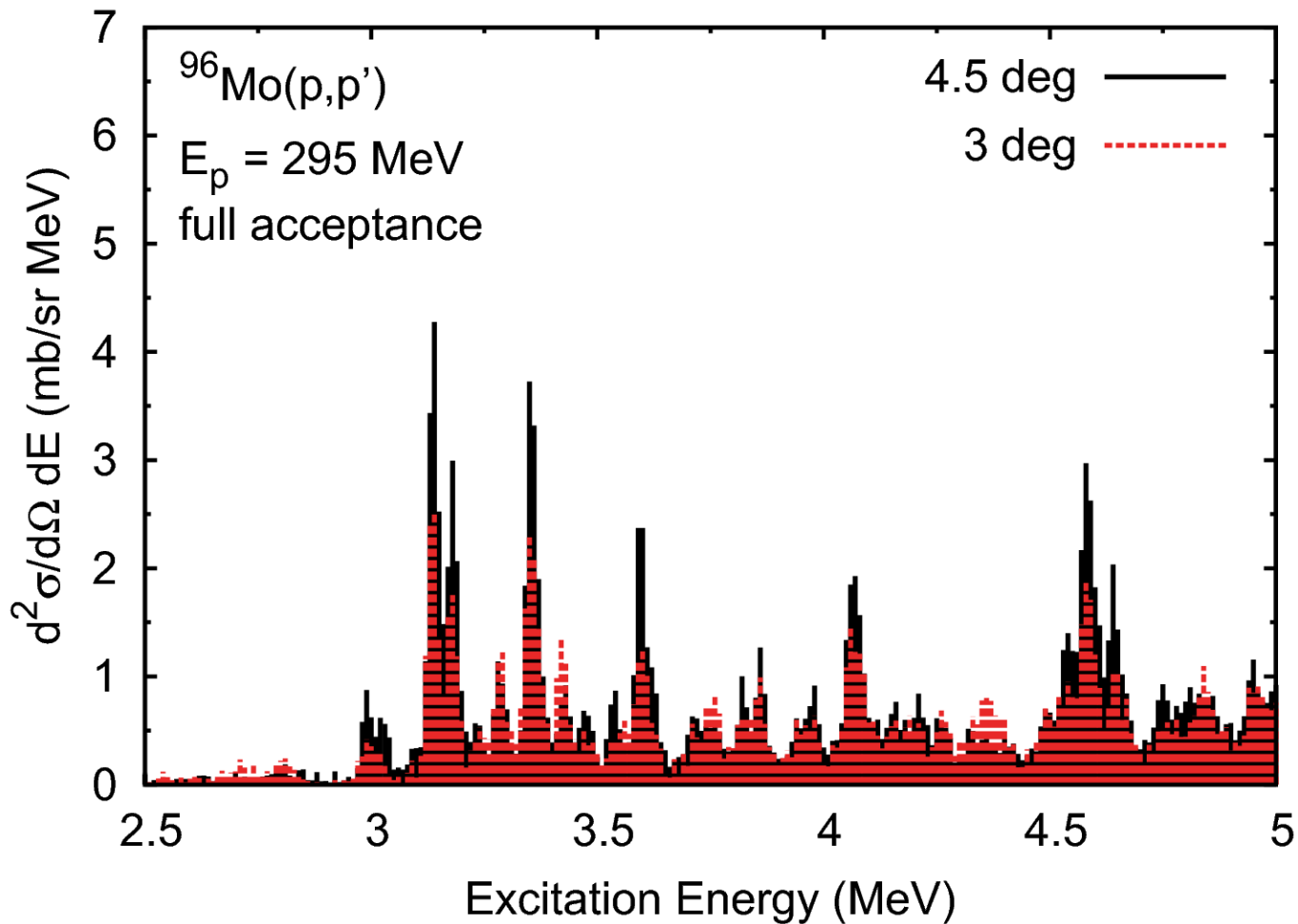
# Appendix 1: 3° spectrum



# Appendix 2: 4.5° spectrum



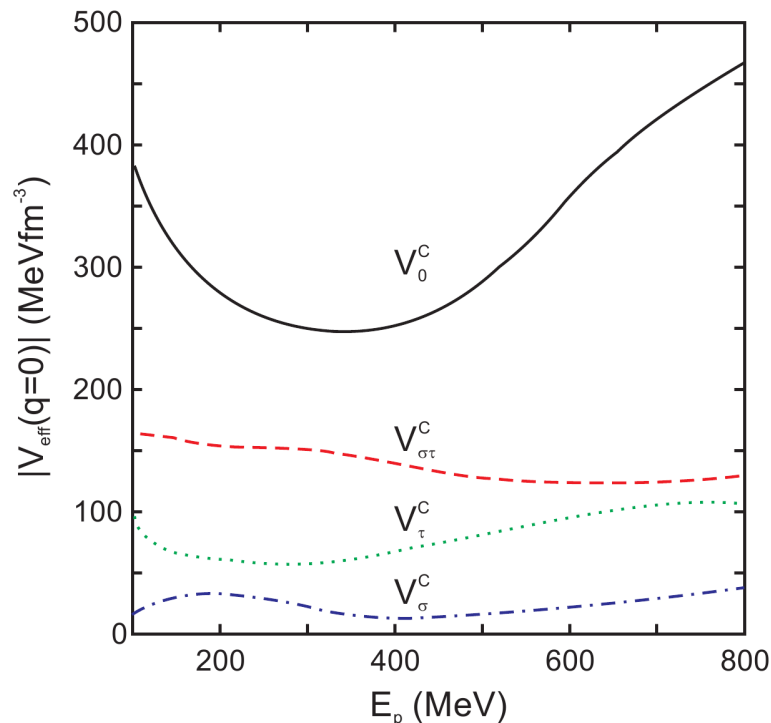
# Appendix 3: 3° and 4.5° spectra



# Appendix 4: Franey-Love interaction

Small momentum transfer: spin-orbit and tensor part of effective interaction negligible:

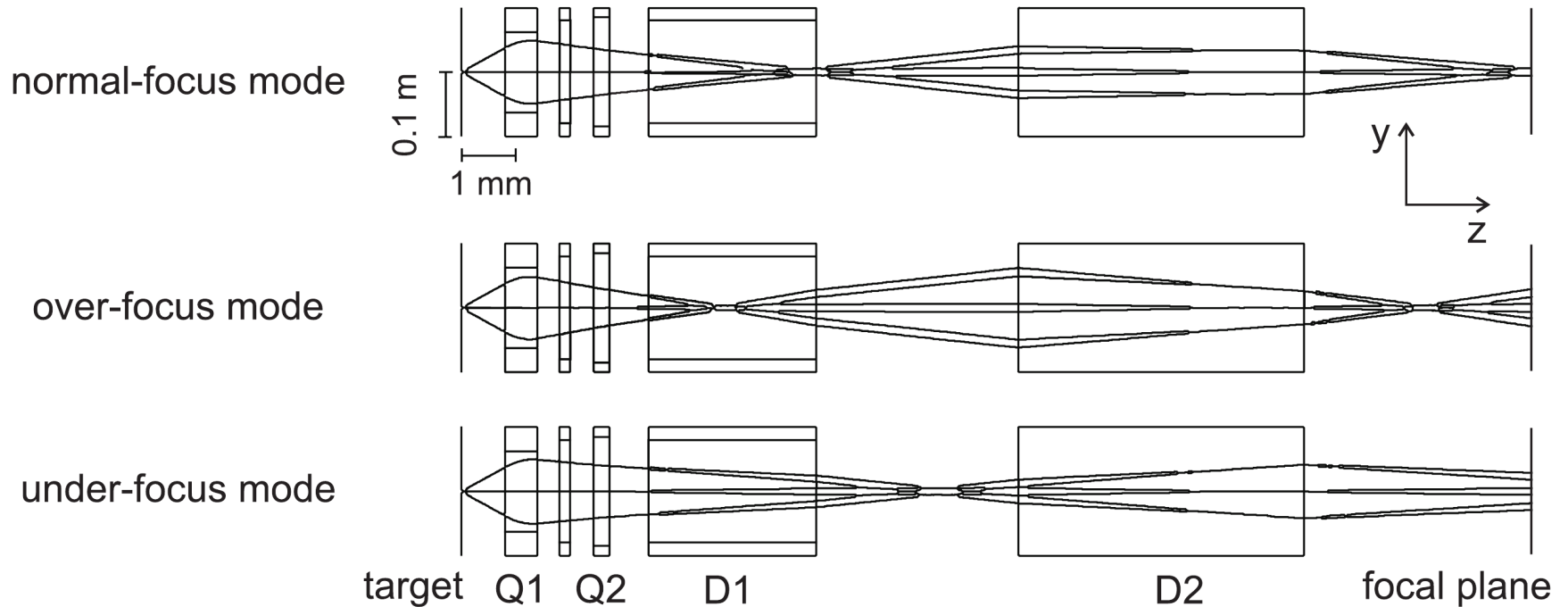
$$V(\vec{r}) = V_0^C(r) + V_\sigma^C(r)\vec{\sigma}_1 \cdot \vec{\sigma}_2 + V_\tau^C(r)\vec{\tau}_1 \cdot \vec{\tau}_2 + V_{\sigma\tau}^C(r)\vec{\sigma}_1 \cdot \vec{\sigma}_2 \vec{\tau}_1 \cdot \vec{\tau}_2$$



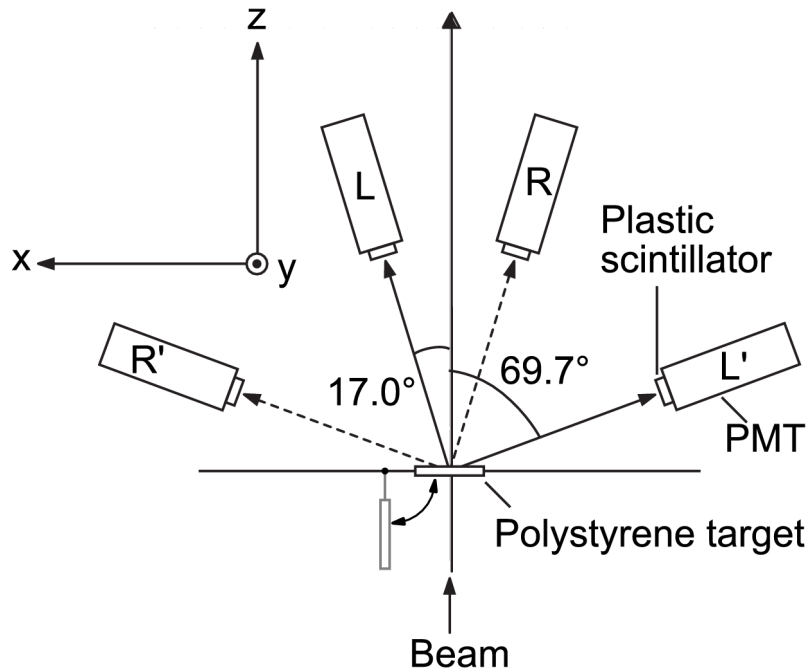
- ▶ Measurements with  $E_p = 300$  MeV
- ▶ Spin-isospin independent term has a minimum
- ▶ Good conditions to observe spin M1 transitions mediated by the spin-isospin dependent part

[W.G. Love and M.A. Franey, PRC **24** (1981) 1073]

# Appendix 5: Focus modes



# Appendix 6: Beam polarization



$$\rho_{N(S)} = \frac{1}{A_y^{BLP}} \frac{1 - X_{N(S)}}{1 + X_{N(S)}}$$

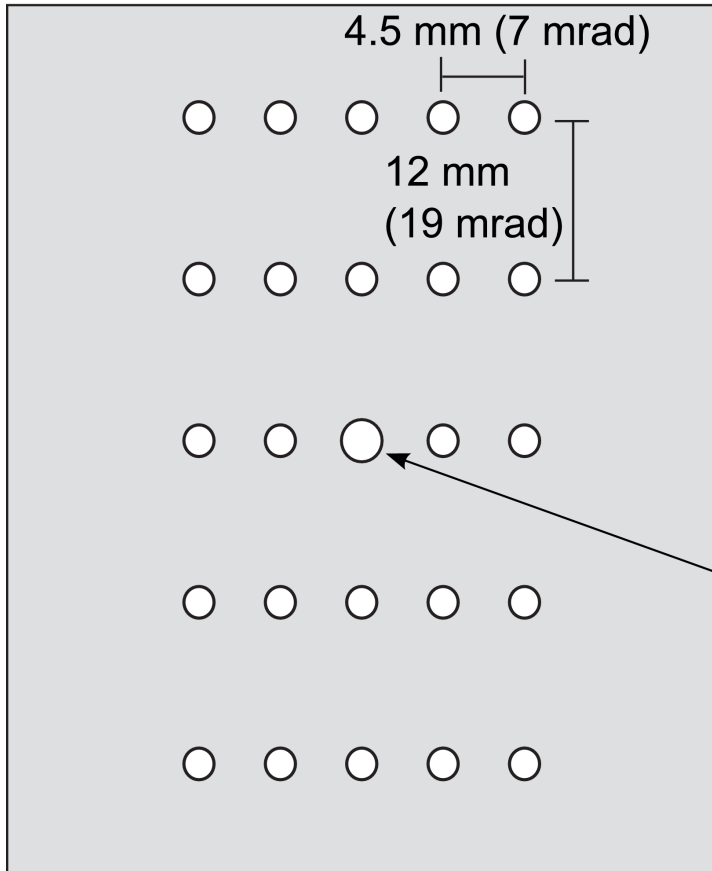
$$X_{N(S)} = \sqrt{\frac{N_{L(D)}^{\uparrow} N_{R(U)}^{\downarrow}}{N_{L(D)}^{\downarrow} N_{R(U)}^{\uparrow}}}$$

$$\rho_N = \rho_N^1 = \rho_N^2$$

$$\rho_S = \rho_S^1$$

$$\rho_L = \frac{\rho_S^1 \cos \chi_{BLP} - \rho_S^2}{\sin \chi_{BLP}}$$

# Appendix 7: Reconstruction of the scattering angles

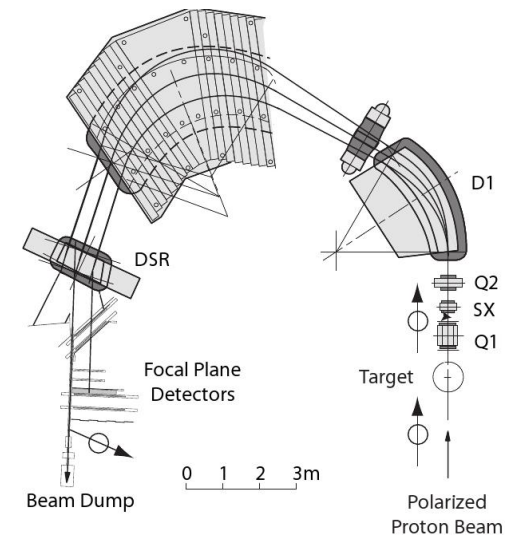


center hole:  
3 mm diameter

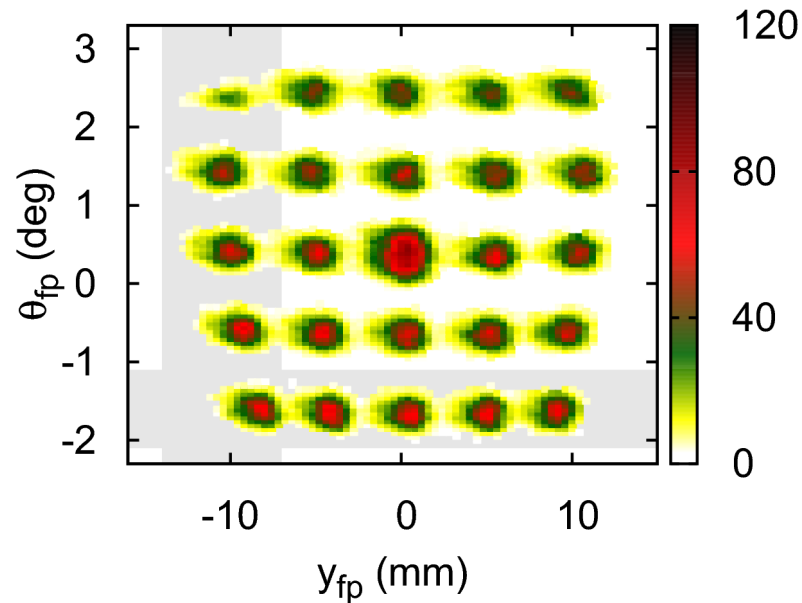
other holes:  
2 mm diameter

material: brass  
thickness: 5 mm

- ▶  $^{58}\text{Ni}$  (100.1 mg/cm<sup>2</sup>)
- ▶  $\theta_{\text{GR}} = 10^\circ$
- ▶ Several settings of the magnetic field
- ▶ Vertical positions: 0,  $\pm 1$  mm



# Appendix 8: Sieve slit analysis

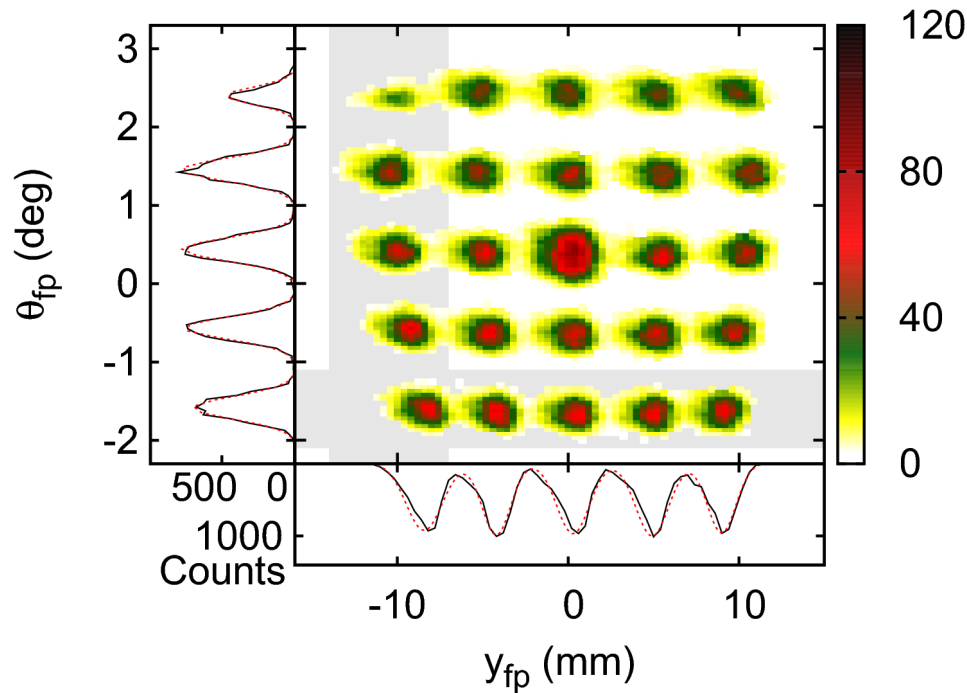


Determination of centers:

- ▶ Plane divided into sectors



# Appendix 8: Sieve slit analysis



Determination of centers:

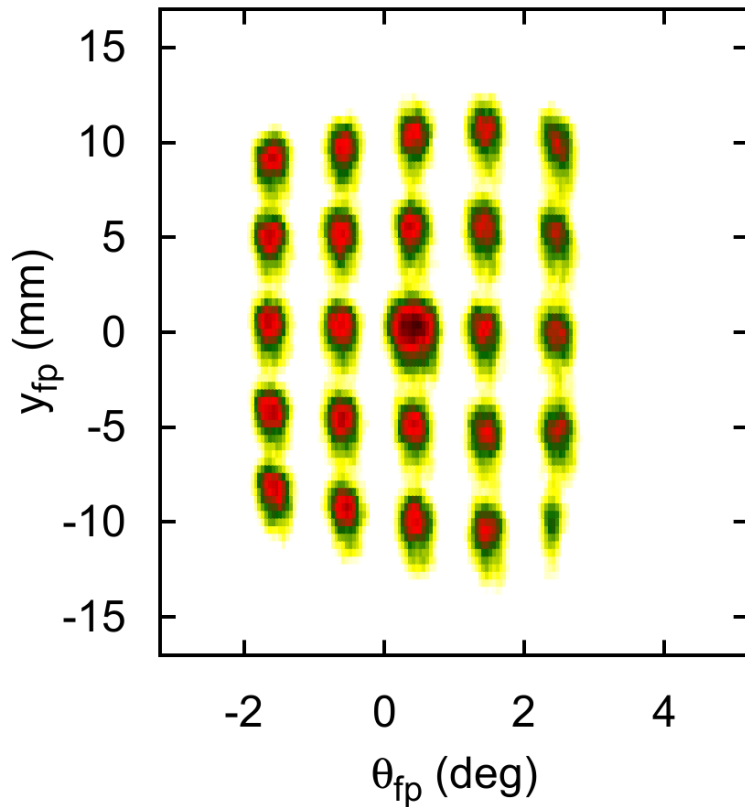
- ▶ Plane divided into sectors
- ▶ Fit with gaussian functions
- ▶ Additionally: established dependences on  $x_{fp}$ ,  $\phi_{fp}$  and  $y_{LAS}$

$$\theta_t(x_{fp}, \theta_{fp}) = \sum_{i=0}^2 \sum_{j=0}^2 a_{ij} \cdot x_{fp}^i \theta_{fp}^j$$

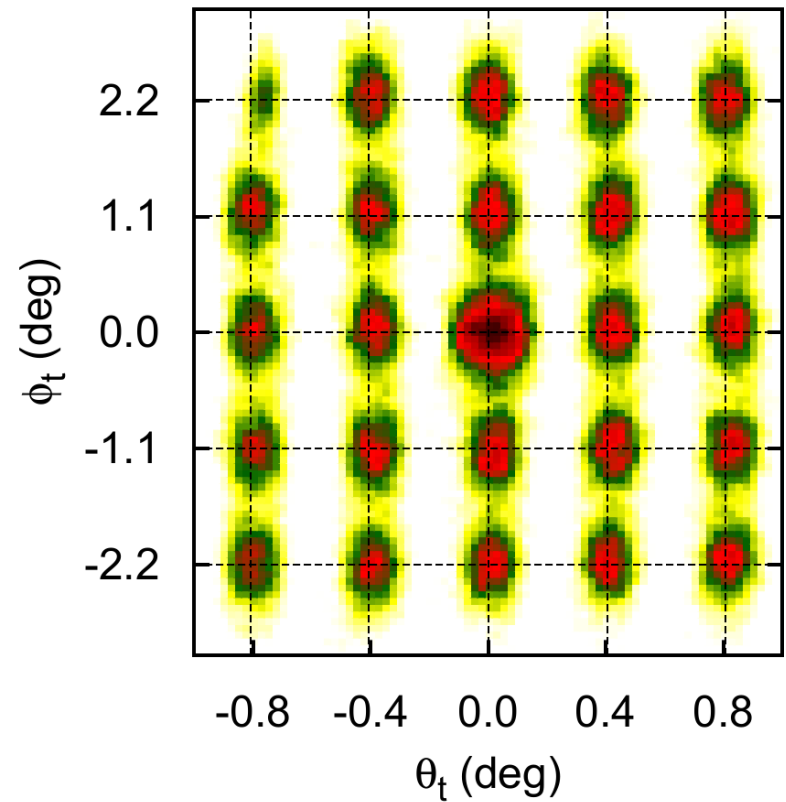
$$\phi_t(x_{fp}, \theta_{fp}, y_{fp}, \phi_{fp}, y_{LAS}) = \sum_{i=0}^2 \sum_{j=0}^2 \sum_{k=0}^2 \sum_{l=0}^2 b_{ijkl} \cdot x_{fp}^i \theta_{fp}^j y_{fp}^k \phi_{fp}^l + \sum_{m=0}^1 c_m \cdot x_{fp}^m y_{LAS}$$

# Appendix 8: Sieve slit analysis

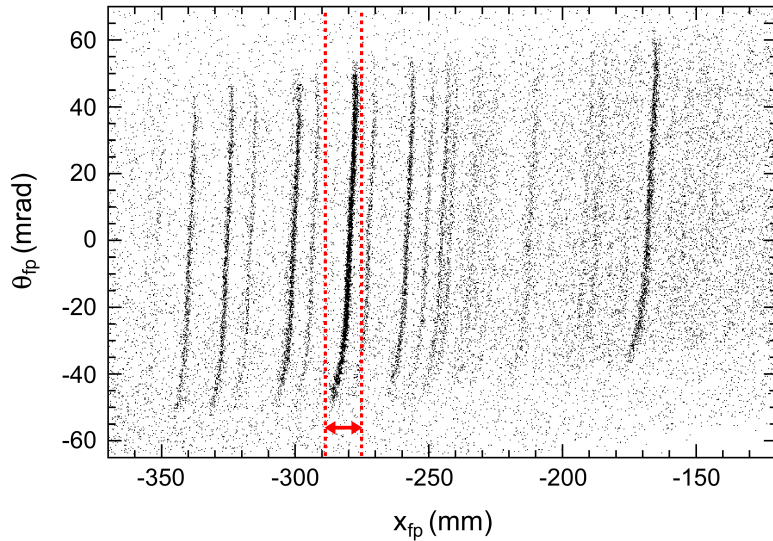
Before



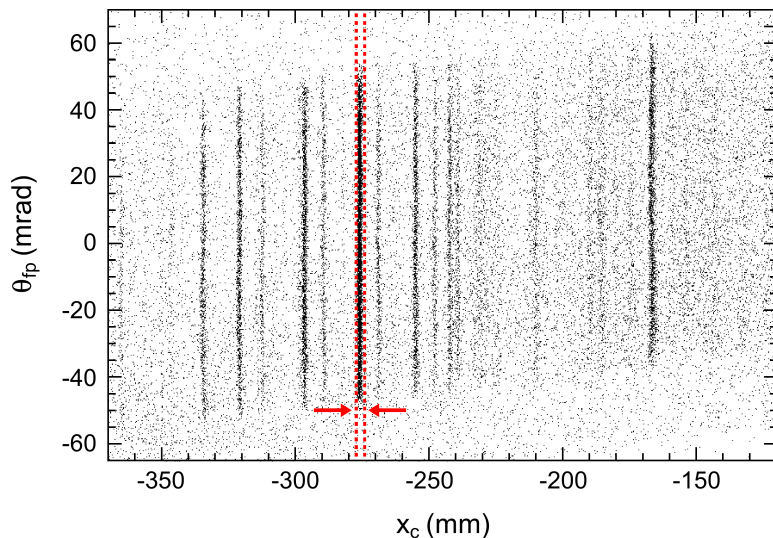
After



# Appendix 9: High-resolution corrections

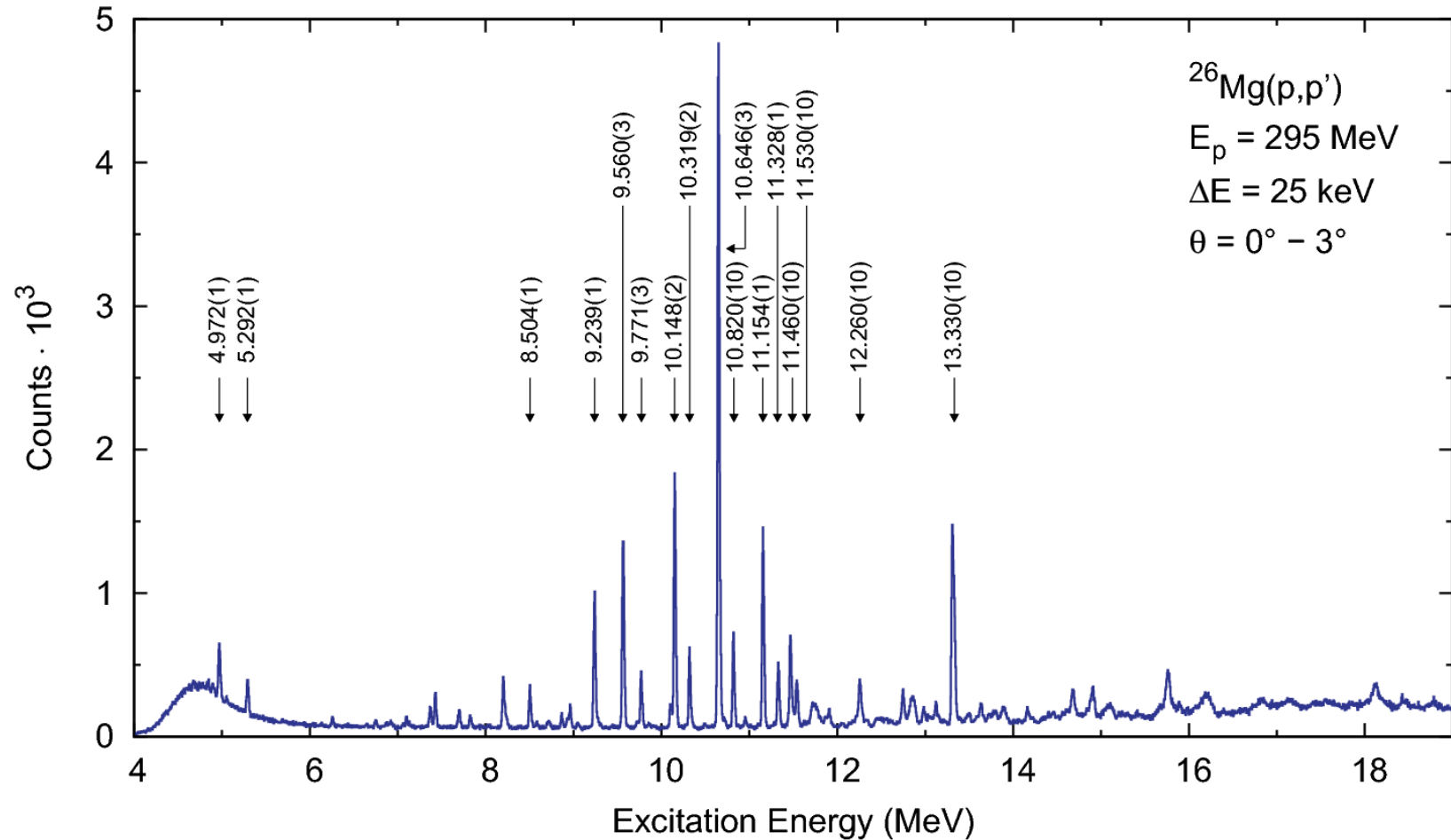


- ▶ Discrete transitions in  $^{26}\text{Mg}$
- ▶ Curved lines in the focal plane
- ▶ Aberration effects ( $\rightarrow$  optics)
- ▶ Polynomial fit:



$$x_c = x_{fp} + \sum_{i=0}^3 \sum_{j=0}^4 d_{ij} \cdot x_{fp}^i \theta_{fp}^j$$

# Appendix 10: Energy calibration



► 2<sup>nd</sup> order polynomial + energy shifts using the highest peak of  $^{26}\text{Mg}$

# Appendix 11: Estimator method

► Effective estimator  $\hat{\epsilon} = \mathbf{F}^{-1} \mathbf{B} = \begin{pmatrix} \hat{\epsilon}_N \\ \hat{\epsilon}_S \end{pmatrix}$  with

$$\mathbf{B} = \begin{pmatrix} \sum_N \cos \phi_{FPP} \\ \sum_N \sin \phi_{FPP} \end{pmatrix}$$

$$\mathbf{F} = \begin{pmatrix} \sum_N \cos^2 \phi_{FPP} & \sum_N \sin \phi_{FPP} \cos \phi_{FPP} \\ \sum_N \sin \phi_{FPP} \cos \phi_{FPP} & \sum_N \sin^2 \phi_{FPP} \end{pmatrix}$$

► Sums over all events

► Calculation of uncertainties with the covariance matrix  $V(\hat{\epsilon}) = \mathbf{F}^{-1}$